DRA

IS NUCLEAR MATTER A QUANTUM CRYSTAL?

V. CANUTO* – S. M. CHITRE†

Institute for Space Studies, Goddard Space Flight Center, NASA, New York

IS NUCLEAR MATTER A QUANTUM CRYSTAL? N73-33656
(NASA) ~~58~~ 61 p HC $5.00 CSCL 20H
Unclas
G3/24 15673

*Also with the Dept. of Physics, City College of New York, N. Y. C.

† NAS-NRC Senior Research Associate
On leave of absence from the Tata Institute of Fundamental Research, Bombay.

ABSTRACT

A possible alternative to the ordinary gas-like computation for nuclear matter is investigated under the assumption that the nucleons are arranged in a lattice. BCC, FCC and HCP structures are investigated. Only HCP shows a minimum in the energy vs. density curve with a modest binding energy of -1.5 MeV. The very low density limit is investigated and sensible results are obtained only if the tensor force decreases with the density. A study of the elastic properties indicates that the previous structures are mechanically unstable against shearing stresses.

I. INTRODUCTION

It can hardly be denied that the problem of nuclear matter represents one of the most difficult and at the same time the most challenging problem in nuclear theory. The principal reason for rather an unsatisfactory solution of this central problem in nuclear physics is that, one's attempts to reproduce the value of the volume energy as close to 17 MeV as possible, have been frustrated largely due to successive improvement of the theory with the tendency nowadays to stabilize around 11.1 MeV. This value was computed by Siemens[1] using the most sophisticated many-body theory now available, namely, the BBP approach.[2] A long way (about 6 MeV) remains to be accounted for, however. In a recent thorough review of the subject, H. Bethe[3] has indicated how contributions of a different nature (none of them being absolutely watertight) can be added to account for just about the missing 5 – 6 MeV. Apart from the uneasiness felt by the process of adding to a good solid number like 11.1 MeV, a less firmly established contribution, the crucial question remains as to whether the theory is actually reliable enough to be considered the appropriate basis for understanding the shell model.

The 5 – 6 missing MeV are too big a chunk to be taken lightly. On the other hand, one could assume the following dichotomic posture: (a) the sought for volume energy is not actually 17 MeV but much less, say about 12 MeV. This possibility was proposed some years ago by one of the authors[4] by showing that summing the energy of a finite nucleus,

$$E \equiv \sum_\alpha \langle\alpha|T + \frac{1}{2} V|\alpha\rangle = \frac{1}{2}\sum_\alpha \epsilon_\alpha + \frac{1}{2}\sum_\alpha \langle\alpha|T|\alpha\rangle$$

upon using a reasonable set of single particle energy levels, ϵ_α an analytic formula was obtained which could in turn be rewritten to exhibit the dependence of the mass formula on A and Z. All the well known terms, namely, volume, surface, asymmetry and Coulomb were obtained. A new term was, however, found to appear with the same sign as the volume energy, whose dependence turned out to be $A^{-2/3}$. The term was shown to contribute $3 \sim 4$ MeV for medium heavy nuclei. The various coefficients were given analytically as functions of parameters usually encountered in the shell model or optical model computations. The overall significance of the computation does not rely on its numerical aspect, but rather on showing that there could still be room for discussion about the proper limit of E/A where $A \to \infty$. (b) A second line of thought was first introduced by Overhauser.[5] He pointed out that a common feature of any many-body treatment is the yet unproven hypothesis that the ground state of a Fermi gas is the familiar sphere of occupied momentum states, instead of, for instance, spatially periodic Hartree-Fock solutions. It therefore remains to be seen if any other type of a single particle wave function could in principle produce a lower energy. Plane wave functions bring out the flavor of a gas, whereas, the abstract concept of nuclear matter could also be thought of as a solid or a liquid. This paper reports the results of a full many-body computation intended to indicate that the nuclear matter is indeed not a solid or a quantum crystal. If it is possible to make a definitive statement about nuclear matter not being in a crystalline state, any extrapolation to liquid structure is of course fraught with many more uncertainties. Liquids are in general, difficult to distinguish from solids in many respects. Liquid Ar,[6] for instance, clearly shows a crystalling structure in its first shell with about 8 neighbors instead of the usual 12 in the close packed structure, when viewed with neutron scattering experiments. Other liquids still show solid-like structure with an increased number of nearest neighbors. The whole concept of a liquid is not clearly understood, as indicated by the partial success achieved by distribution function theories and by Lennard-Jones-

Devonshire theory[7] that reproduce reasonably well the data, even though their starting point is quite different. The only clear-cut definition upon which nobody disagrees is that liquids do not possess any ability to resist shear stresses whereas solids do.

This mechanical definition is of fundamental importance in the following sense. Suppose one computes the ground state energy of a many-body system of nucleons by using, instead of plane waves, wave functions such as Bloch wave functions or Wannier functions and finds that the energy at the nuclear density turns out to be less than the one yielded by the corresponding gas-like computation. From that result it would be quite premature to conclude that the solid structure necessarily represents the actual state of affairs. The mechanical properties of the solid have to be tested. The lower energy state can turn out to be totally unstable against shearing stresses, i.e., one has to make sure that the elastic constants of the medium do not go soft. M. Born[8] has given a series of criteria to decide as to whether the ordered structure melts, evaporates or goes into an intermediate state similar to plastic or "gel."

We have attempted three different ordered structures: BCC (body-centered cubic), FCC (face-centered cubic) and HCP (hexagonal close packing). In the three cases, the system was shown to be mechanically unstable against shearing stresses, or put in a different way, the significant elastic constant went soft for the density integral between 10^{12} gr/cc $\leqslant \rho \leqslant 4 \times 10^{14}$ gr/cc. One can therefore conclude quite safely that the idealized N = Z infinite system at $\rho \cong 3.\ 10^{14}$ gm/cm^3 is surely not in any of the most commonly encountered solid state structure. On energetic grounds it turns out that the binding energy per particle E/N has a minimum of - 1. 5 MeV at 2. 842 10^{14} gr/cc for the HCP structure whereas for BCC and FCC the problem of the existence of a minimum is much harder to discern.

II. THE MANY-BODY TREATMENT

The many-body treatment used is an extension of the T-matrix approach to quantum crystals (solid He^3) recently discussed by Brandow.[9] An excellent review can be found in a paper by Guyer[10].

The Slater determinant for a system of N particles is built up by single particle wave functions of the form

$$\phi(r) = \alpha^{3/2}\, \pi^{-3/4}\, e^{-(\alpha^2/2)\,|r-R|^2} \qquad (1)$$

where R is the coordinate of the lattice site around which the particle is supposed to perform an oscillatory motion under the combined influence of the remaining (N-1) particles. Equation (1) is the eigenfunction of an harmonic oscialltor potential U(r), centered around the lattice site R, i.e.,

$$U(r) = \frac{1}{2} m\omega^2 (r-R)^2 \quad . \tag{2}$$

The frequency ω (which cannot exceed the Debye frequency ω_D at zero temperature) enters in the wave function (1) through the parameter $\alpha^{-1} = (m\omega/\hbar)^{-\frac{1}{2}}$ that represents the spread of ϕ around the lattice site. At the present stage of the computation such a parameter is as yet unknown and plays a fundamental role in the theory. Some remarks about the explicit form (1) are quite in order. One is accustomed to think that a wave function of a particle in a crystal should possess the periodicity of such a crystal or equivalently be a Bloch function. To begin with, the HF equations are highly non-linear and if one starts with a ϕ of that form one will not necessarily end up with such a form after the desired convergence has been achieved. In the second place, any linear combination of Bloch functions is still a solution; such a linear combination can turn out to possess quite a high degree of localization (such as Wannier functions) of the form given in eq. (1). Evidently one of the prices paid by not actually performing such a linear combination of Bloch functions is represented by the fact that the parameter ω is unknown. The troubles encountered in not making such a consideration and bodily considering ϕ as a trial function with α as a variational parameter are too well known in solid He^3 not to be repeated here. Nosanow and co-worker have determined α from HF.[12] We have followed the same spirit in our calculation, i.e., we take the single particle potential to be given by

$$U(r_1) = \sum_j \int \phi_j^*(r_2)\, V(r_1-r_2)\, \phi_j(r_2)\, d^3r_2 \qquad (3)$$

where the two-body nucleon-nucleon potential is taken to be Reid's phenomenological soft-core potential. The sum over j indicates the sum over the successive neighbor distances (shells) from a given particle located at R_1 in an arbitrary system of coordinates. The values of ω (or α) obtained by solving eq. (3) are then used to start the full HF equations which finally give the final form of ϕ. The angular momentum decomposition of $V(r_1-r_2)$ complicates life quite a bit and it was found that the following decomposition was very useful

$$\frac{e^{imR}}{R} = \frac{\pi i}{2\sqrt{r\rho}} \sum_{\ell=0}^{\infty} (2\ell+1) J_{\ell+1/2}(m\rho) H^{(1)}_{\ell+1/2}(mr) P_\ell(\cos\varphi) \qquad \rho < r$$

with $R^2 = r^2 + \rho^2 - 2r\rho\cos\varphi$ (and on equivalent expression for $r < \rho$).

Reid's potential is in its most important part a superposition of Yukawa's. The structural nature of the specific crystal BCC, FCC or HCP enters when the summation over j has to be performed. Depending upon the density, the sum was performed over as many neighbors as necessary to ensure a satisfactory convergence. At nuclear density the number is about 5 — 6, whereas at much higher densities, say $\rho \geq 10^{15}$ gr/cc, one has to sum over at least 36 neighbors. The values of α^{-1}, the spread of the single particle wave function vs. ρ (density) are given in Tables 1, 3, 5 together with the first neighbor distance. Each particle spreads about 30% of the distance of the lattice site, an excursion quite acceptable even on the basis of an empirical rule such as the one often encountered: The crystal melts whenever the oscillations reaches a sizable fraction of the lattice constant (Lindeman rule). Even though this criterion can be easily seen not to have general validity (to have a semi-quantitive basis, zero point oscilllations are very large and yet do not induce any melting)our spread is well within the safety margin for each nucleon to perform comfortable excursion from its lattice site. We should perhaps remark that Lindeman's rule can be derived in many alternative ways.

A major complication arises in the nuclear case because of the possible spin configurations: given a structure, say BCC, one could in principle arrange the protons and neutrons in practically an infinite number of ways depending upon the spin configuration. In a BCC structure one has two interpenetrating cubes amounting to 16 sites, 8 for neutrons and 8 for protons; the configuration is still infinitely degenerate with respect to spin arrangements. One could start with any site of a cube with, say, a neutron with its spin up; in the next site on the same cube one can put N↑, N↓, P↓ or P↑. In the next point one again has the same degeneracy and so on. One can come up with the most asymmetrical configuration with three consecutive particles with spin ↑, then two with spin ↓ and thus randomly distributed as far as the unit cell is concerned. We have tried many of them with an arbitrary degree of randomness just to insure that they are not energetically convenient. It was then established that this was indeed the case and that: for a given configuration the minimum was achieved whenever the spins (of neighboring particles on the same cube) were symmetrically arranged, half with spin up and half with spin down.*

---

* Natura non facit saltus (Lucretius, de Rerum Natura).

An analagous situation was found to hold for the other two configurations studied, namely FCC and HCP. In the usual nuclear matter computation one sums over all the possible spin orientations, an operation that is not allowed in a discretized structure such as an ordered arrangement. This will explain why the energy per particle formula looks different from the one that is usually displayed in Brueckner formulation.

The many-body formulation used here is the same that has been quite successfully applied to solid He^3, or for that matter, to any quantum crystal. The main difference will be in the angular momentum decomposition of the two-body wave function, say ψ. In the solid He^3 case, the formulation includes only $l=0$ waves since the Leonard-Jones potential is assumed to be a $l=0$ state. This is not at all obvious and the authors[12] have recently shown that a much better agreement with the experimental data can be achieved if one allows the He^3 atoms to interact also in $l=1, 2$ states. In principle, it is difficult to fully understand a wave function decomposed into angular momentum waves upon considering that the Y_ℓ^m are related to a sphere, whereas the particles are located spatially with a cubic symmetry for BCC and FCC, and hexagonal symmetry for HCP. On the other hand the phenomenological nucleon-nucleon potential now in extensive use is given explicitly for each $^{2S+1}L_J$ wave and one is therefore forced to decompose the wave function into Y_ℓ^m . About this point one could sophisticate a little bit more by considering how the potential itself is deduced from the S-matrix. Reid potential is not strictly under this jurisdiction since it is supposed to have been deduced upon fitting scattering data and deuteron properties. Even then the general basic structure is written down on the pionic theory. When one deduces $V(x)$, one essentially Fourier-transforms the second order of the S-matrix which in turn makes use of the Dirac free spinors. Evidently this is not the case in a crystal structure where the nucleons would have a relativistic harmonic-oscillator wave function (which do not exist) as a spinor. The use of a free two-nucleon potential could in principle be questionable but this is the best one can do at the present time.

The actual computation of E/N has been reviewed elsewhere and we will therefore only quote the results. Since the original Slater determinant is made up of displaced harmonic oscillator wave functions, the kinetic energy will evidently be

$$E_{K.E.} = \frac{3}{4}\frac{\hbar^2}{m}\alpha^2 N \tag{4}$$

The potential energy has a familiar form too, namely,

$$E_{P.E.} = \sum_{i<j} \frac{\int \Phi(ij)\, V(ij)\, \Psi(ij)\, d^3x_j\, d^3x_i}{\int \Phi(ij)\, \Psi(ij)\, d^3x_j\, d^3x_i} \tag{5}$$

where Φ is the free two-body wave function, i.e., $\Phi(r_1 r_2) = \phi(r_1)\phi(r_2)$, whereas $\Psi(r_1 r_2)$ is the correlated or perturbed wave function which we have to study. Transforming to relative and center of mass coordinates, expression (5) becomes

$$E_{P.E.} = \frac{1}{2} N \sum_{\Delta} N_{\Delta} \frac{\int \Phi(r)\, V(r)\, \Psi(r)\, d^3r}{\int \Phi(r)\, \Psi(r)\, d^3r} = \frac{1}{2} N \sum_{d} N_d \varepsilon_d \tag{6}$$

where N_Δ is the number of particles at distance Δ from the one chosen as the origin. In any non-T-matrix approach, like in the Jastrow variational method, one does not have at this point an equation for ψ of the same form as the one we are about to present. The form of $E_{P.E.}/N$ is also different since a logarithmic term is added to the potential. Among the various degrees of sophistication that one can use to write down the equation for ψ, we shall make use of the one first employed by Guyer and Zane,[13] i.e.,

$$\left[T_1 + T_2 + U(1) + U(2) + V(12)\right]\psi(12) = \mathcal{E}\,\psi(12) \tag{7}$$

which is physically easy to understand. T(1) and T(2) are, respectively, the kinetic energies; U(1) and U(2), the harmonic oscillator potentials of particles 1 and 2; and V(12), the two-body interaction potential. Equation (7) is the equation of motion of two particles, each of them moving in an harmonic potential centered around two different points, and, in addition, interacting through a two-body potential. When the two harmonic potentials are centered at the same point (in particular, $R_1 = R_2 = 0$), the problem simplifies greatly and it was studied in connection with shell model computations by Nigam[14] some years ago. Equation (7) is the most difficult equation to solve. Once ψ is known, the energies can easily be calculated. If one uses for U(1) and U(2) the form (2), equation (7) becomes

$$\left\{-\frac{\hbar^2}{2M}\nabla_R^2 - \frac{\hbar^2}{2\mu}\nabla_r^2 + \frac{1}{2}\omega^2\left(m_1R_1^2 + m_2R_2^2\right) + \frac{1}{2}\mu\omega^2 r^2 - \mu\omega^2\vec{r}\cdot\vec{\Delta} + V(r)\right\}\Psi = \mathcal{E}\Psi \tag{8}$$

where $\mu = \dfrac{m_1m_2}{m_1+m_2}$, $M = m_1 + m_2$, $r = r_1 - r_2$, $R = \dfrac{m_1r_1 + r_2m_2}{M}$.

At this point it is usually assumed that $\Psi = \phi(1)\phi(2)g(r)$: if, on one side, it is quite a pictorial way of stating that Ψ differs from

Φ by a $g(r)$ (correlation function), on the other side, it has quite a disastrous consequence if one filters $\phi(1)\phi(2)$ to the left side of eq. (8) (as is usually done), leaving an equation only for $g(r)$. Equation (8) as such, contains, after introducing $\Psi^* = \Psi/r$, only second derivatives, whereas the process of filtering $\phi(1)\phi(2)$ to the left, introduces a first derivative which cannot be eliminated: from the numerical point of view this is highly undesirable, as we have found by personal experience. As a matter of fact, the only computation that has made use of the equation for $g(r)$ instead of for Ψ itself,[15] shows that the boundary conditions were more difficult to meet. If, moreover, the potential $V(r)$ has an angular dependence, then the transportation of $\phi(1)\,\phi(2)$ to the left is totally illegal, since the remaining $g(r)$ would still have to be decomposed into partial waves, thus,

$$g(r) = \sum_{\ell} g_{\ell}(r)\;\; Y_{\ell}(\Omega) \tag{9}$$

without the possibility of giving any physical significance to ℓ whatsoever, since part of the physical angular momentum (most of it!) contained in $\phi(1)\,\phi(2)$ has been transported to the left. To be more specific, a matrix element of the form

$$\int Y_{\ell}^{*}(\Omega)\;\; V(\vec{r})\, V_{\ell'}\;(\Omega)\; d\Omega$$

with ℓ and ℓ' defined by eq. (9), would be completely meaningless. Since in the nuclear case, V(r) is highly angular-momentum dependent, the only choice is to write the full angular momentum decomposition of Ψ as

$$\Psi(r) = \sum_{\ell=0}^{\infty} \sum_{J} (2\ell+1) i^{\ell} \sqrt{\frac{4\pi}{2\ell+1}} \left(\ell 0 S M_S \,|\, J M_S\right) \sum_{\ell'} \Psi_{\ell\ell'}^{JS}(r)\, \mathcal{Y}_{\ell' JS}^{M_S}(\vec{r}, \vec{d}) \tag{10}$$

in obvious notation. The second summation over ℓ' is introduced to take into account the presence of tensor forces. Equation (8) contains a cos θ term which (much like the Stark effect) couples ℓ with $\ell \pm 1$. It does not couple different spins and therefore it is to be expected that ${}^1S_0$, ${}^1P_1$, ${}^1D_2$ will be correlated by such a term, and analogously the triplet states ${}^3S_1$, ${}^3\tilde{S}_1$, ${}^3P_0$, ${}^3P_1$, ${}^3P_2$, ${}^3D_1$, ${}^3\tilde{D}_1$, ${}^3D_2$ will be linked together through the solid state term. After substituting eq. (10) into eq. (8) and performing a long angular momentum algebra, the results are ($x = r/r_0$, $d = \Delta/r_0$, $a = \alpha r_0$):

SINGLET

$$\begin{cases} h_0'' + (E - U_0)h_0 + a(x,d)h_1 = 0 \\ h_1'' + (E - U_1)h_1 + \frac{1}{3}a(x,d)\left[h_0 - 2h_2\right] = 0 \\ h_2'' + (E - U_2)h_2 - \frac{2}{5}a(x,d)h_1 = 0 \end{cases} \tag{11}$$

where the following notation has been used

$$^1S_0: \quad r\psi^{00}_{00} \equiv h_0 \qquad a(x,d) = \frac{1}{2}a^4 xd$$

$$^1P_1: \quad r\psi^{10}_{11} = h_1$$

$$^1D_2: \quad r\psi^{20}_{22} = h_2$$

TRIPLET

$$h_3'' + (E-U_3)h_3 - \sqrt{8}\, V_T \frac{2\mu r_0^2}{\hbar^2} \tilde{h}_3 + \frac{1}{9} a(x,d)\left[h_4 + 3h_5 + 5h_6\right] = 0$$

$$\tilde{h}_3'' + (E-\tilde{U}_3)\tilde{h}_3 - \sqrt{8}\, V_T \frac{2\mu r_0^2}{\hbar^2} h_3 - \frac{\sqrt{2}}{9} a(x,d)\left[h_4 - \frac{3}{2}h_5 + \frac{1}{2}h_6\right] = 0$$

$$h_4'' + (E-U_4)h_4 + \quad 0 \quad + \frac{1}{3}a(x,d)\left[\left(h_3 + \sqrt{2}\,\tilde{h}_7\right) - \sqrt{2}\left(\tilde{h}_3 + \sqrt{2}\,h_7\right)\right] = 0$$

$$h_5'' + (E-U_5)h_5 + \quad 0 \quad + \frac{1}{3}a(x,d)\left[\left(h_3 - \frac{1}{\sqrt{2}}\,h_7\right) + \frac{1}{\sqrt{2}}\left(\tilde{h}_3 - \frac{1}{\sqrt{2}}\,h_7\right) - \frac{3}{2}h_8\right] = 0$$

$$h_6'' + (E-U_6)h_6 + \quad 0 \quad + \frac{1}{3}a(x,d)\left[\left(h_3 + \frac{1}{5\sqrt{2}}\,\tilde{h}_7\right) - \frac{1}{5\sqrt{2}}\left(\tilde{h}_3 + \frac{1}{5\sqrt{2}}\,h_7\right) - \frac{3}{10}h_8\right] = 0$$

$$h_7'' + (E-U_7)h_7 - \sqrt{8}\, V_T \frac{2\mu r_0^2}{\hbar^2} \tilde{h}_7 - \frac{1}{9}a(x,d)\left[2h_4 + \frac{3}{2}h_5 + \frac{1}{10}h_6\right] = 0$$

$$\tilde{h}_7'' + (E-\tilde{U}_7)\tilde{h}_7 - \sqrt{8}\, V_T \frac{2\mu r_0^2}{\hbar^2} h_7 + \frac{\sqrt{2}}{9}a(x,d)\left[h_4 - \frac{3}{2}h_5 + \frac{1}{2}h_6\right] = 0$$

$$h_8'' + (E-U_8)h_8 - \quad 0 \quad - \frac{1}{10}a(x,d)\left[3h_5 + h_6\right] = 0 \tag{12}$$

with the following notation

$$
\begin{array}{llll}
{}^3S_1: & r\psi^{11}_{00} = h_3 & {}^3P_2: & r\psi^{21}_{11} = h_6 \\
{}^3\tilde{S}_1: & r\psi^{11}_{02} = \tilde{h}_3 & {}^3D_1: & r\psi^{11}_{22} = h_7 \\
{}^3P_0: & r\psi^{01}_{11} = h_4 & {}^3\tilde{D}_1: & r\psi^{11}_{20} = \tilde{h}_7 \\
{}^3P_1: & r\psi^{11}_{11} = h_5 & {}^3D_2: & r\psi^{21}_{22} = h_8
\end{array}
\tag{13}
$$

The potentials U_k and $\tilde{U}_k$ are given by

$$
\begin{aligned}
U_k &= \frac{1}{4} a^4 x^2 + \frac{2\mu r_0^2}{\hbar^2} V_k + \frac{\ell(\ell+1)}{x^2} \\
\tilde{U}_3 &= \frac{1}{4} a^4 x^2 + \frac{2\mu r_0^2}{\hbar^2} V\left({}^3D_1\right) + \frac{6}{x^2} \\
\tilde{U}_7 &= \frac{1}{4} a^4 x^2 + \frac{2\mu r_0^2}{\hbar^2} V\left({}^3S_1\right)
\end{aligned}
\tag{14}
$$

The two-body potentials V_k are taken from Reid.[15]

As one can see, the equations are intrinsically coupled by the solid state term a(x, d\). Only two normalization conditions are therefore necessary: one for the singlets and one for the triplets.

The solution of the 3 + 8 equations has presented us with major numerical difficulties; no simple theorem of the Sturm-Liouville form exist for coupled equations and the search for the ground state energy was indeed a painful and delicate process.

The major concern was to make sure that the h_k's had no nodes or else that the energy eigenvalues being computed were actually the lowest. In problems of stellar evolution and in studies of turbulence, equations of this nature frequently arise, but with the major difference that seldom any eigenvalue problem has to be handled; the energy E is just a prescribed parameter.

Given a certain Δ (first neighbor distance) and α^{-1} (spread of the wave function) we found that around the nuclear density†

---

† $\rho = nm, \qquad n = \frac{4}{r_{FCC}^3}, \frac{2}{r_{BCC}^3}, \frac{\sqrt{2}}{r_{HCP}^3}; \quad r_{FCC} \equiv r_0$

---

the 3 + 8 solutions were behaving very well; by that we mean that the maximum of the h's was at the proper neighboring distance, Δ. The shape of h_k is essentially a gaussian as seen in the figures below; this is to be expected since Ψ differs from Φ by a correlation function that doesn't usually change the shape. The location of the h's is very important since the energy of the system is proportional to hV; classically hV is just V computed at exactly the lattice site since the wave functions are all delta functions, i.e., when $\alpha \rightarrow \infty$, $\phi \rightarrow \delta\ (r_1 - R_1)$. Quantum mechanically, besides the location of the peak determined by the 3 + 8 equation, each h has a certain spread, α^{-1}. For the same r , if Δ increases the h's have a tendency to lag behind.

We have tried three possible configurations: BCC, FCC and HCP. The geometrical disposition of neutrons and protons as well as the energy per particle are given below for each case.

Energy Expressions

As mentioned earlier, the energy expressions depend on the spin arrangements. We will therefore have to distinguish among several cases. Using Eq. (6) and the definition of ψ as given by (10), the various possibilities are

N↑, N↑ (OR P↑ P↑)

$$\epsilon_1 = \frac{\int_0^\infty a(x) j_1 \left\{h_6 V_6 + h_5 V_5\right\} dx}{\int_0^\infty a(x) j_1 \left\{h_6 + h_5\right\} dx}$$

N↑, N↓ (OR P↑ P↓)

$$\epsilon_2 = A \frac{\int_0^\infty a(x)[j_0 V_0 h_0 + 5 j_2 V_2 h_2] dx}{\int_0^\infty a(x)[j_0 h_0 + 5 j_2 h_2] dx} + (1-A) \frac{\int_0^\infty a(x) j_1 [2h_6 V_6 + h_4 V_4] dx}{\int_0^\infty a(x) j_1 [2h_6 + h_4] dx}$$

N↑, P↑

$$\epsilon_3 = B \frac{\int_0^\infty a(x) j_1 [h_6 V_6 + h_5 V_5] dx}{\int_0^\infty a(x) j_1 [h_6 + h_5] dx} +$$

$$+ C \frac{\int_0^\infty a(x) \left[j_0 h_3 V_3 + j_0 \bar{h}_3 V_T + \frac{5}{2} j_2 \left(h_8 V_8 + \frac{h_7 V_7}{5} + \frac{\bar{h}_7 V_T}{5} \right) - \frac{1}{\sqrt{2}} \left(j_0 \bar{h}_7 V_3 + j_0 h_7 V_T + j_2 h_3 V_t + j_2 \bar{h}_3 V_7 \right) \right] dx}{\int_0^\infty a(x) \left[j_0 h_3 + \frac{5}{2} j_2 \left(h_8 + \frac{1}{5} h_7 \right) - \frac{1}{\sqrt{2}} \left(j_0 \bar{h}_7 + j_2 \bar{h}_3 \right) \right] dx}$$

N↑, P↓

$$\epsilon_4 = D \frac{\int_0^\infty a(x)\, j_1 [h_1 V_1] dx}{\int_0^\infty a(x)\, j_1 [h_1] dx} + E \frac{\int_0^\infty a(x) [j_0 h_0 V_0 + 5 j_2 h_2 V_2] dx}{\int_0^\infty a(x) [j_0 h_0 + 5 j_2 h_2] dx} + F \frac{\int_0^\infty a(x)\, j_1 [2h_6 V_6 + h_4 V_4] dx}{\int_0^\infty a(x)\, j_1 [2h_6 + h_4] dx}$$

$$+ G \frac{\int_0^\infty a(x) [j_0 h_3 V_3 + j_0 \bar{h}_3 V_T + 2 j_2 h_7 V_7 + 2 j_2 \bar{h}_7 V_T + \sqrt{2}(j_0 \bar{h}_7 V_3 + j_0 h_7 V_T + j_2 h_3 V_T + j_2 \bar{h}_3 V_7)] dx}{\int_0^\infty a(x) [j_0 h_3 + 2 j_2 h_7 + \sqrt{2}(j_0 \bar{h}_7 + j_2 \bar{h}_3)] dx}$$

As explained before, only two normalization constants are required. They are simply determined by requiring that each energy denominator should be normalized to unity in conformity with the man-body theory requirement that

$$\int \Phi \cdot \psi \, d^3 r = 1 \quad .$$

The explicit forms of the constants A, B, C, D, E, F are finally obtained and since they do not present any interest per se they have not been written down here.

The remaining quantities are defined as

$$a(x) = xe^{-a^2 x^2/4} \quad ; \qquad y = \frac{1}{2} a^2 xd$$

$$j_0 = \frac{1}{y} \sinh y \quad ; \quad j_1 = \frac{1}{y} \cosh y - \frac{1}{y^2} \sinh y \quad ; \quad j_2 = \frac{3}{y^2} \cosh y - \left(\frac{1}{y} + \frac{3}{y^3}\right) \sinh y$$

The origin of the Bessel functions (of imaginary argument) can be easily understood. When, in Eq. (5), we write the product of $\phi(1)\phi(2)$ for $\Phi(ij)$ the result contains a term of the form

$$\exp\left(\frac{\alpha^2}{2} \vec{r} \cdot \vec{\Delta}\right)$$

which, when expanded in plane wave in a form analogous to Eq. (10), gives

$$\chi_S^{M_S} \, e^{(\alpha^2/2)\vec{r} \cdot \vec{\Delta}} = \sum_{\lambda, J}^{\infty} i^{\lambda} \sqrt{4\pi(2\lambda+1)} \; j_{\lambda}\left(-i \frac{\alpha^2 r \Delta}{2}\right) \mathcal{Y}_{\lambda JS}^{M_S} \left(\vec{r} \cdot \vec{\Delta}\right)$$

if only $h_0 \neq 0$ one easily recovers the expression for the energy used by Massey and Woo[16] in their study of solid He^3.

If we sum up all the energy expressions, i. e., we sum over the spin orientation, we recover the familiar expression of Brueckner theory.

III. RESULTS

B. C. C. Structure

The geometrical disposition of the nucleons is shown in Figure 1. Out of a plethora of possibilities, the one given below was found to minimize the energy. In Table 1 we present the results: the first column gives the density; the second the appropriate lattice parameter; the third the location of the first neighbor; the fourth the spread of the wave-functions; then the kinetic, potential and total energy per particle follow in order.

TABLE 1

$\rho \times 10^{14}$ (g/cc)	r_{BCC} (f)	Δ (f)	α^{-1} (f)	KE (MeV)	PE (MeV)	E/N (MeV)
1.045	3.175	2.75	1.04	28.63	-28.90	-0.2744
2.842	2.274	1.97	0.73	57.61	-54.95	+2.667
3.96	2.037	1.76	0.65	74.18	-66.54	+7.642

At nuclear density $\rho = 2.842 \times 10^{14}$ gr/cm^3, the system is unbound with E/N = + 2.667 MeV. To appreciate the nature of the wave-functions we list below in Table 2 the distance in fermis where they peak at the various densities and the first neighbor distance around which they should peak.

TABLE 2

LOCATION OF THE PEAK OF THE WAVE FUNCTIONS (in fermis)

$\rho \times 10^{14}$ (g/cc)	r_{BCC} (f)	$^1S_0$	$^1P_1$	$^1D_2$	Δ (f)	$^3S_1$	$^3\tilde{S}_1$	$^3P_0$	$^3P_1$	$^3P_2$	$^3D_1$	$^3\tilde{D}_1$	$^3D_2$
1.045	3.175	2.28	2.79	2.81	2.74	1.651	1.64						
3.96	2.037	1.63	1.87	1.95	1.76	1.38	1.14	1.79	1.71	1.73	1.4	1.42	1.72

Here, too, at the nuclear density $\rho = 2.84 \times 10^{14}$ gr/cm^3, the system is unbound with an energy of +.5936 MeV. We have also added the values of E/N for much lower ρ where the peak h's occur at an nonphysical distance. It is seen that at $r_{FCC} = 10f$, or $\rho = 6.69 \times 10^{12}$ gr/cm^3, the potential energy is -8.01 which is clearly absurd. The reason can be easily understood by looking at Table 4, where we present the location of the peaks of the various h's (compared to where it should) for different densities. The situation becomes disastrous at lower densities and this explains the unrealistic negative energy.

In Figures 3 – 18 we display the h's at $r_{FCC} = 2.566$ for two distances $\Delta = 1.81f$ (first shell), and $\Delta = 9.07f$ (24th shell), and also exhibit the corresponding potentials in the combination hV. It is seen that the location of the peak is excellent for $\Delta = 1.81f$, whereas at $\Delta = 9.07$, the h's lag behind. This is of no particular consequence since the contributions of the 24th shell are minute.

Since at low densities the wave-functions are not reliable, the energy minimum that appears in the curve of E/N vs. ρ (Table 3) is not to be trusted. One possible source of error could be attributed to the HF; we therefore moved α quite arbitrarily

TABLE 4

LOCATION OF THE PEAK OF THE WAVE FUNCTIONS (in fermis)

ρ (gr/cc)	r_{FCC} (f)	$^1S_0$	$^1P_1$	$^1D_1$	Δ (f)	$^3S_1$	$^3\tilde{S}_1$	$^3P_0$	$^3P_1$	$^3P_2$	$^3D_1$	$^3\tilde{D}_1$	$^3D_2$
6.69×10^{12}	10.	5.7	6.6	7.5	7.07	1.5	1.2	5.7	5.1	4.8	1.2	1.5	6.6
2.43×10^{13}	6.5	3.5	4.48	4.87	4.59	1.56	1.36	4.09	3.9	3.7	4.48	1.56	4.48
5.35×10^{13}	5.	1.85	3.45	3.75	3.53	1.65	1.35	3.3	3.15	2.85	3.45	1.5	3.45
1.04×10^{14}	4.	2.28	2.88	3.12	2.82	1.68	1.32	2.76	2.52	2.4	2.76	1.44	2.88
2.84×10^{14}	2.866	1.805	2.15	2.23	2.02	1.46	1.20	2.06	1.89	1.80	1.97	1.29	2.06
3.96×10^{14}	2.566	1.64	1.95	1.95	1.815	1.44	1.13	1.85	1.745	1.64	1.85	1.23	1.85

into two opposite directions: in both cases the results either did not change appreciably or became more disastrous. A close inspection of Table 4 shows that the misbehavior in the 8-equations is much more pronounced than in the system of 3. Among the triplets waves, $^3P_0$, $^3P_1$, $^3P_2$ and $^3D_2$ still behave reasonably well whereas $^3S_1$, $^3\tilde{S}_1$, $^3D_1$ and $^3\tilde{D}_1$ grossly misbehave. The reason can be seen to be the uneven presence of the tensor force in Eq. (12): $^3P_0$, $^3P_1$, $^3P_2$ and $^3D_2$ do not contain V_T in the same way as the others do; we therefore arbitrarily put $V_T = 0$ at low density. The situation improved quite remarkably. The h's were having the maximum at the expected positions. This procedure seemed to indicate that the tensor force should contain a density dependent factor, say $f(\rho)$, equal to one at $\rho = \rho_{\text{nucl.}}$ which decreases when ρ decreases. Since only one point on the curve is known, $\rho = \rho_{\text{nucl.}}$, one cannot hope to determine the form of the function. The fact that at low density the values of E/N are misbehaving is not at all surprising if we consider that the explicit form of the nucleon-nucleon potential used here has been fitted to data at the nuclear density and not any lower. The argument is of general nature and one therefore would be led to think that not only V_T is affected, but all the remaining parts of the potential. This is surely true, but a low densities the s-waves are dominant and their misbehavior is more important than any other wave; consequently the tensor force that couples $^3S_1$ and $^3D_1$ plays a particularly significant role.

HCP Structure

A more interesting case is presented by the HCP structure. It is known from solid state physics that in many instances when an FCC structure ceases to exist as a result of some of its elastic constants going soft, the crystal structure most frequently does not melt but, rather, shears into an HCP structure. It was therefore natural to consider the possible alternative. The geometry is shown in Fig. 19. The energy results are given in Table 5.

TABLE 5

ρ (gr/cc)	r_{HCP} (f)	Δ (f)	α^{-1} (f)	K. E. (MeV)	P. E. (MeV)	E/N (MeV)	E/N (V_T = 0) (MeV)
3.1×10^{13}	4.243	4.243	1.57	12.56	-12.06	+0.4998	8.48
5.35×10^{13}	3.536	3.536	1.334	17.43	-17.51	-0.0811	10.60
1.04×10^{14}	2.828	2.828	1.067	27.23	-27.35	-0.1232	
2.84×10^{14}	2.026	2.026	0.765	53.04	-54.55	-1.5	
3.96×10^{14}	1.8151	1.8151	0.672	68.64	-66.42	+2.219	

31-A ##

TABLE 6

LOCATION OF THE PEAK OF THE WAVE FUNCTIONS (in fermis)

ρ (gr/cc)	r_{HCP} (f)	$^1S_0$	$^1P_1$	$^1D_2$	Δ (f)	$^3S_1$	$^3\tilde{S}_1$	$^3P_0$	$^3P_1$	$^3P_2$	$^3D_1$	$^3\tilde{D}_1$	$^3D_2$
6.69×10^{12}	7.07	5.51	6.78	7.42	7.07	1.7	1.27	5.73	5.3	5.1	6.6	1.5	6.6
3.1×10^{13}	4.24	3.4	4.1	4.4	4.24	1.7	1.4	3.9	3.6	3.4	4.1	1.5	4.1
5.35×10^{13}	3.53	2.7	3.5	3.8	3.53	1.7	1.3	3.3	3.1	2.9	3.5	1.5	3.5
1.04×10^{14}	2.83	2.26	2.83	3.05	2.83	1.58	1.24	2.7	2.6	2.4	2.7	1.5	2.83
2.84×10^{14}	2.03	1.78	2.1	2.3	2.03	1.46	1.22	2.03	1.9	1.8	2.03	1.3	2.1
3.96×10^{15}	1.815	1.66	1.89	2.03	1.81	1.45	1.16	1.89	1.74	1.6	1.815	1.3	1.89

Again the situation becomes unrealistic as soon as the h's start peaking at an unphysical distance. We have also included the case $V_T = 0$. The situation regarding the location is markedly improved at very low density, whereas it is probably over-estimated in the intermediate region where the join-up should be smoother. In Table 6 we report the location of the peaks for the various h's. The HCP, undoubtedly presents a distinctive characteristic with respect to BCC and FCC. For the density region where the wave-functions are still acceptable, namely in the lower part of the table, the energy E/N vs. ρ has a minimum at exactly the nuclear density. It is very slightly bound -1.5 MeV.

IV. ELASTIC CONSTANTS

We have stressed in the Introduction that the system of neutrons and protons arranged in a lattice structure must be tested for stability against deformations. There have been several attempts to derive criteria for melting of a solid, the well known amongst which is Lindemann's rule. This rule is based on the assumption that a solid melts when the amplitude of oscillation of a vibrating particle is a sizable fraction of the nearest neighbor distance. Such an empirical criterion can only be regarded as a convenient "rule of thumb" designed to test semi-quantitatively the stability of a crystalline structure and indeed, a complete theory of melting must necessarily examine the detailed stability of a lattice when it is deformed under shearing stresses.

Any lattice has to satisfy the requirement that its energy density must have a stationary value at equilibrium. However, for the structure to be stable, the energy must have a positive definite quadratic form, thus leading to an increase in its value when undergoing a small strain. For the purpose of investigating the mechanical stability of a crystal lattice we consider a cube with side 2a which is deformed homogeneously into a parallelepiped whose sides are the vectors $\vec{r}_1$, $\vec{r}_2$, $\vec{r}_3$. Thus the lattice points of the undistorted cube which are described by

$$\vec{R}_o = \left(\ell_1 a, \ \ell_2 a, \ \ell_3 a\right)$$

are now given by the vectors

$$\vec{R}_\delta = \ell_1\vec{r}_1 + \ell_2\vec{r}_2 + \ell_3\vec{r}_3$$

where the integers ℓ_1, ℓ_2, ℓ_3 assume different sets of values for the B. C. C., F. C. C. lattices. Now for small deformation the square of the distance from the origin is given by

$$R^2 = R_o^2 + a^2 \sum_{\alpha\beta} e_{\alpha\beta}\, \ell_\alpha \ell_\beta = R_o^2 + \delta \quad , \tag{16}$$

where $e_{\alpha\beta}$ are the strain components of the theory of elasticity:

$$e_{11} = \frac{r_1^2 - a^2}{a^2} \ , \qquad e_{22} = \frac{r_2^2 - a^2}{a^2} \ , \qquad e_{33} = \frac{r_3^2 - a^2}{a^2} \ ,$$

$$e_{23} = \frac{\vec{r}_2 \cdot \vec{r}_3}{a^2} \ , \quad \text{etc.}$$

The total potential energy E of a lattice where the interparticle forces are only central, may be written as

$$E/N = \frac{1}{2}\sum \Phi\left(\sqrt{R_o^2 + \delta}\right)$$

But since for any function $\Phi(r)$ we have

$$\frac{d}{d\delta}\, \Phi\left(\sqrt{R_o^2 + \delta}\right) = \left(\frac{1}{r}\frac{d}{dr}\,\Phi\right)_{r=\sqrt{R_o^2+\delta}} \equiv \left(D\Phi\right)_{r=\sqrt{R_o^2+\delta}} \quad ,$$

we may express $\Phi(r)$ in a Taylor series:

$$\Phi\left(\sqrt{R_o^2+\delta}\right) = \Phi\left(R_o\right) + \delta\left(D\Phi\right)_{R_o} + \frac{1}{2}\,\delta^2\left(D^2\Phi\right)_{R_o} + \ . \ . \ . \quad ,$$

and hence the potential energy can be written as

$$(E/N)_\delta = \frac{1}{2}\sum\left\{\Phi + \delta D\Phi + \frac{1}{2}\delta^2 D^2\Phi + \ldots\right\} \tag{17}$$

$$= (E/N)_o + \frac{a^2}{4}\sum_{\alpha\beta} e_{\alpha\beta}\ell_\alpha\ell_\beta D\Phi + \frac{a^2}{16}\sum_{\alpha\beta\mu\nu} e_{\alpha\beta}e_{\mu\nu}\ell_\alpha\ell_\beta\ell_\mu\ell_\nu D^2\Phi + \ldots$$

Here the first term on the right-hand side is the energy of the undeformed cube which will be neglected hereafter; the second term is zero at equilibrium while the last term may be rewritten as

$$(E/NV)_\delta = \frac{1}{2}\, c_{11}\left(e_{xx}^2 + e_{yy}^2 + e_{zz}^2\right) + c_{12}\left(e_{yy}e_{zz} + e_{zz}e_{xx} + e_{xx}e_{yy}\right)$$

$$+ \frac{1}{2}c_{44}\left(e_{yz}^2 + e_{zx}^2 + e_{xy}^2\right) \quad , \tag{18}$$

with

$$c_{11} = \frac{2a}{\gamma}\quad \sum D^2\,\Phi\ell_1^{\,4} - P \ ,$$

$$c_{12} = \frac{2a}{\gamma}\quad \sum D^2\,\Phi\ell_1^2\ell_2^2 \ ,$$

$$c_{44} = \frac{2a}{\gamma}\sum D^2\,\Phi\ell_1^2\ell_2^2 - P \ ,$$

$$\gamma = 4(BCC) \ , \quad \gamma = 2(FCC) \ , \quad V = \gamma a^3 \ ,$$

and the summation extends over successive shells.

If we now identify R with Δ_d , the distance from the origin of various shells, we can compute, numerically, the first and second derivatives of the potential energy at successive shell distances and sum over a desired number of shells (in order to achieve convergence) and evaluate the elastic constants c_{11} and c_{12} as a function of the matter density ρ. The crystalline structure is considered stable if $(E/NV)_\delta > 0$, i.e., if there is a gain in energy while undergoing a deformation. It is straightforward to show that the quadratic form (18) is positive-definite provided the following conditions are satisfied:

$$c_{11} + 2c_{12} > 0 \ ,$$

$$c_{44} > 0 \ ,$$

$$c_{11} - c_{12} > 0 \ .$$

Physically it is clear that the elastic constant c_{44} represents the shear modulus as it multiplies that part of the deformation energy which is proportional to the non-diagonal terms, e_{yz}, e_{zx},

For computing the elastic constants we follow the procedure outlined by Born(8) and the results for nuclear matter arranged in an FCC lattice are (in units of 10^{35} dynes/cm^2):

$c_{11} = -2.83 \qquad c_{44} = -.71 \qquad r_{FCC} = 2.57\text{f} \ , \quad \rho = 3.96 \times 10^{14}\ \text{gm/cm}^3$

$c_{11} = -1.79 \qquad c_{44} = -.48 \qquad r_{FCC} = 2.86\text{f} \ , \quad \rho = 2.84 \times 10^{14}\ \text{gm/cm}^3$

thus indicating a complete mechanical instability of the system. Here the pressure P is very small compared to the $C'_{\alpha\beta}$ and hence $C_{12} \cong C_{44}$.

For a BCC structure the corresponding elastic constants again come out to be negative and the system is evidently mechanically unstable. We thus conclude that nuclear matter is unlikely to exist in any of the commonly occurring crystalline structures.

V. CONCLUSIONS

None of the most common solid-state structures seem to be an even probable candidate to represent what is known as nuclear matter. The conventional BCC and FCC configurations very likely do not even give a minimum in the energy curve, or, if they do so, it would be in a density region much lower than the usual nuclear matter density. However, HCP does have a minimum at $\rho = \rho_{\text{nucl.}} = 2.842 \times 10^{14}$ gm/cm^3 with a modest binding of energy of -1.5 MeV, about a factor of ten lower than the experimental value.

In conclusion, a solid-state structure does not seem to be a better alternative to the usually employed gas computation.

It remains to be seen what an actual liquid type of computation would do. Due to the great difficulties already encountered in the theory of classical liquids, an extension of that formalism to include complicated angular and spin dependent nuclear forces does not seem to be just around the corner.

REFERENCES

1) P. Siemens, Nucl. Phys. A141 (1970) 225

2) H. A. Bethe, B. H. Brandow, and A. G. Petschek, Phys. Rev. 129 (1963) 225

3) H. A. Bethe, Ann. Rev. of Nucl. Science, ed. E. Segré, Vol. 21 (1971)

4) M. Bauer and V. Canuto, Arkiv för Fyski, 36 (1967) 393

5) A. W. Overhauser, Phys. Rev. 4 (1960) 415

6) J. de Boer, Progress in low temperature Physics, ed. C. J. Gorter, Vol. II (North-Holland, Amst., 1957)

7) J. A. Barker, Lattice Theories of the Liquid State (The MacMillan Co., New York, N. Y., 1963)

8) M. Born and K. Huang, Dynamic Theory of Crystal Lattices (Oxford, 1950) 129 ff.

9) B. H. Brandow, Ann. of Phys., 1972, to be published

10) R. A. Guyer, Solid State Phys., ed. D. Turnbull, Vo. 23 (1969) 413

11) L. H. Nosanow, Phys. Rev. 146 (1966) 120

12) V. Canuto and S. Chitre, A new approch to quantum solids, (1972) preprint

13) R. A. Guyer and I. Zane, Phys. Rev. 188 (1969) 445

14) R. Nigam, Phys. Rev. B138 (1964) 133

15) R. V. Reid, Ann. of Phys. 50 (1968) 411

16) W. E. Massey, and C. W. Woo, Phys. Rev. 196 (1968) 241

FIGURE CAPTIONS

Fig. 1: The B.C.C. arrangement for an equal number of neutrons and protons

Fig. 2: The F.C.C. arrangement for an equal number of neutrons and protons

Fig. 3: The singlet $\ell = 0$ wave-functions h vs. r at a given density.

The peak is very pronounced and it is around the first neighbor distance.

Fig. 4: Same as in Fig. 3 for the triplet, $\ell = 0$ case.

Fig. 5: Same as in Fig. 3 for the triplet, $\ell = 1$ case.

Fig. 6: Same as in Fig. 3 for the triplet, $\ell = 2$ case.

Fig. 7: The product hV vs. r [$\psi(^1S_o) \equiv h_o$ etc.] for singlet even.

Fig. 8: The product hV vs. r for the mixed terms.

Fig. 9: The product hV vs. r for the triplet odd case.

Fig. 10: The product hV vs. r for the triplet even case.

Fig. 11 - 18: The same as for Fig. 3 - 10 for the 24th shell.

It can be seen that the wave-functions lag behind, i.e., they do not peak quite at the appropriate Δ. This brings too much attraction into the energy. Fortunately the contribution of such a distant shell is negligible.

Fig. 19: The H.C.P. configuration for equal number of neutrons and protons.

ACKNOWLEDGMENTS

The authors wish to thank Mal Ruderman, E. Salpeter and E. Spiegel each for asking different but enlightening questions. One of us (S. M. C.) would like to thank Dr. R. Jastrow for his hospitality at the Institute for Space Studies.

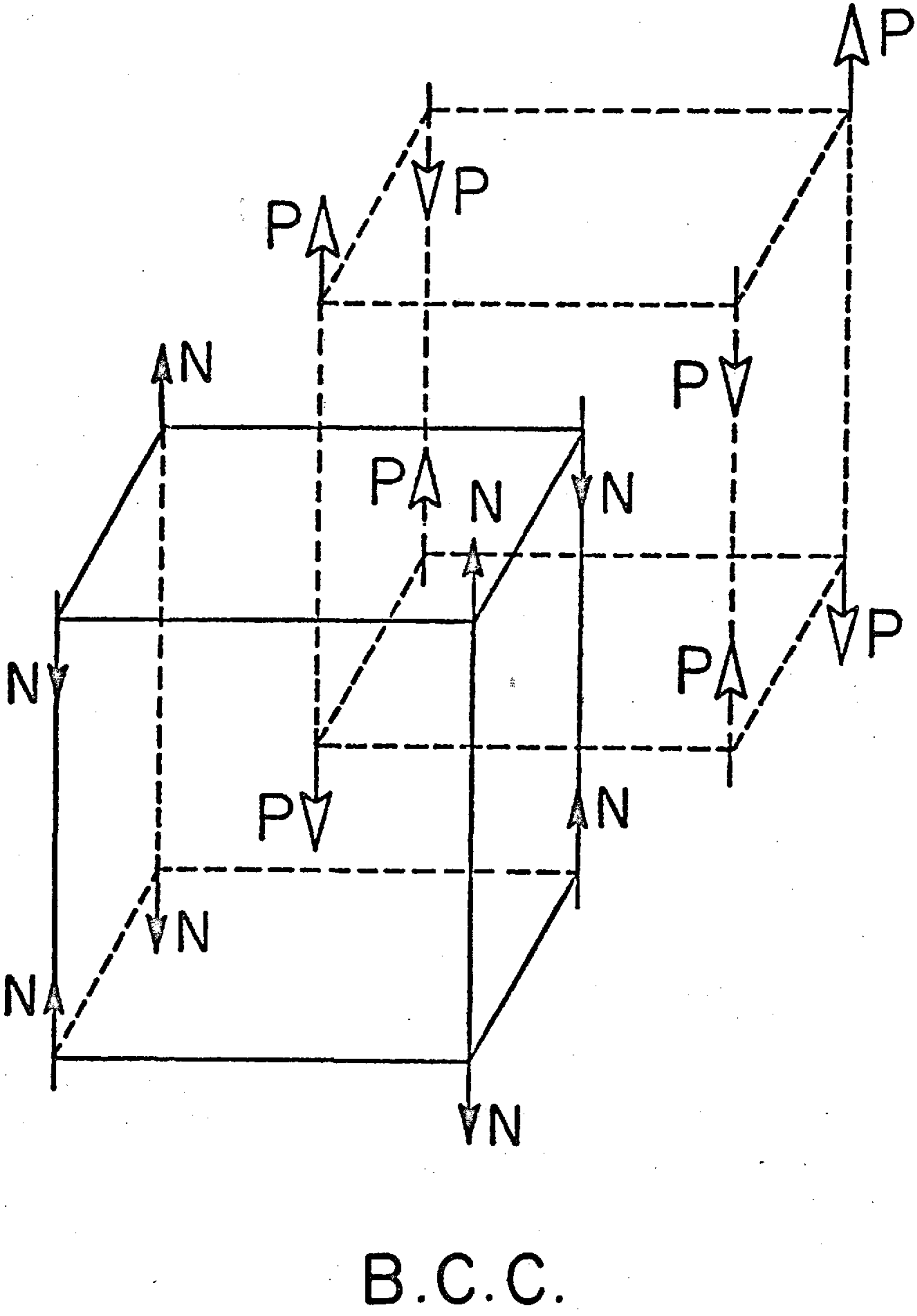

Fig. 1

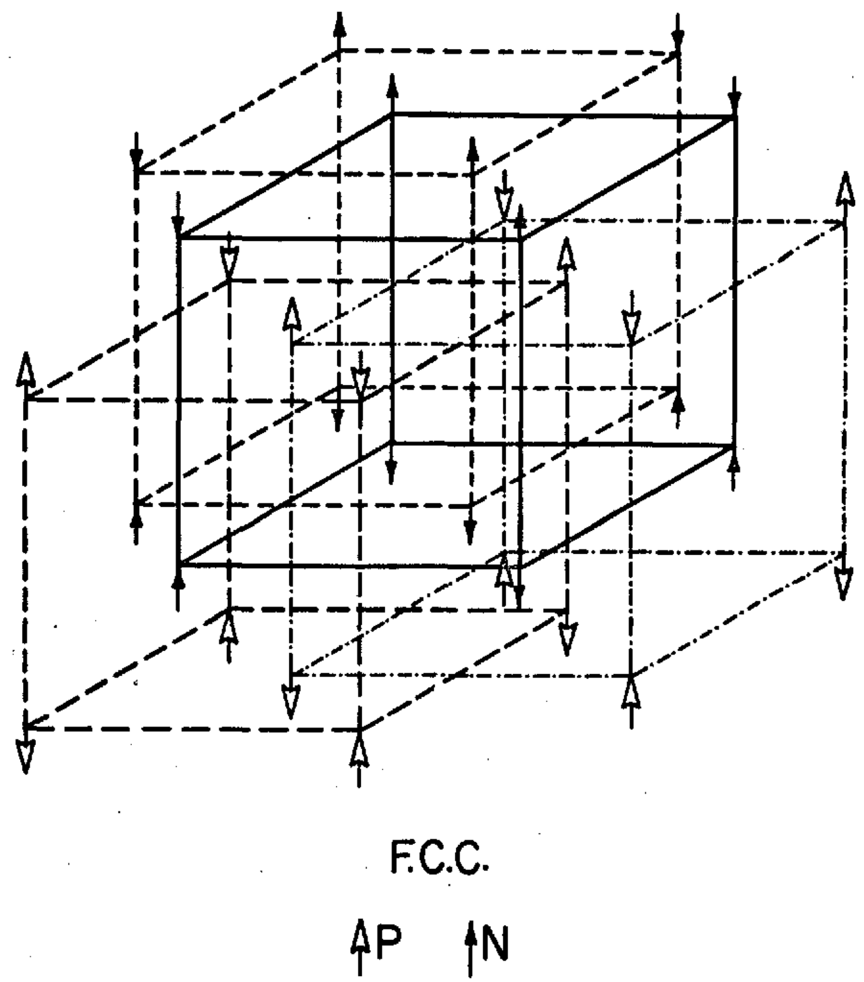

Fig. 2

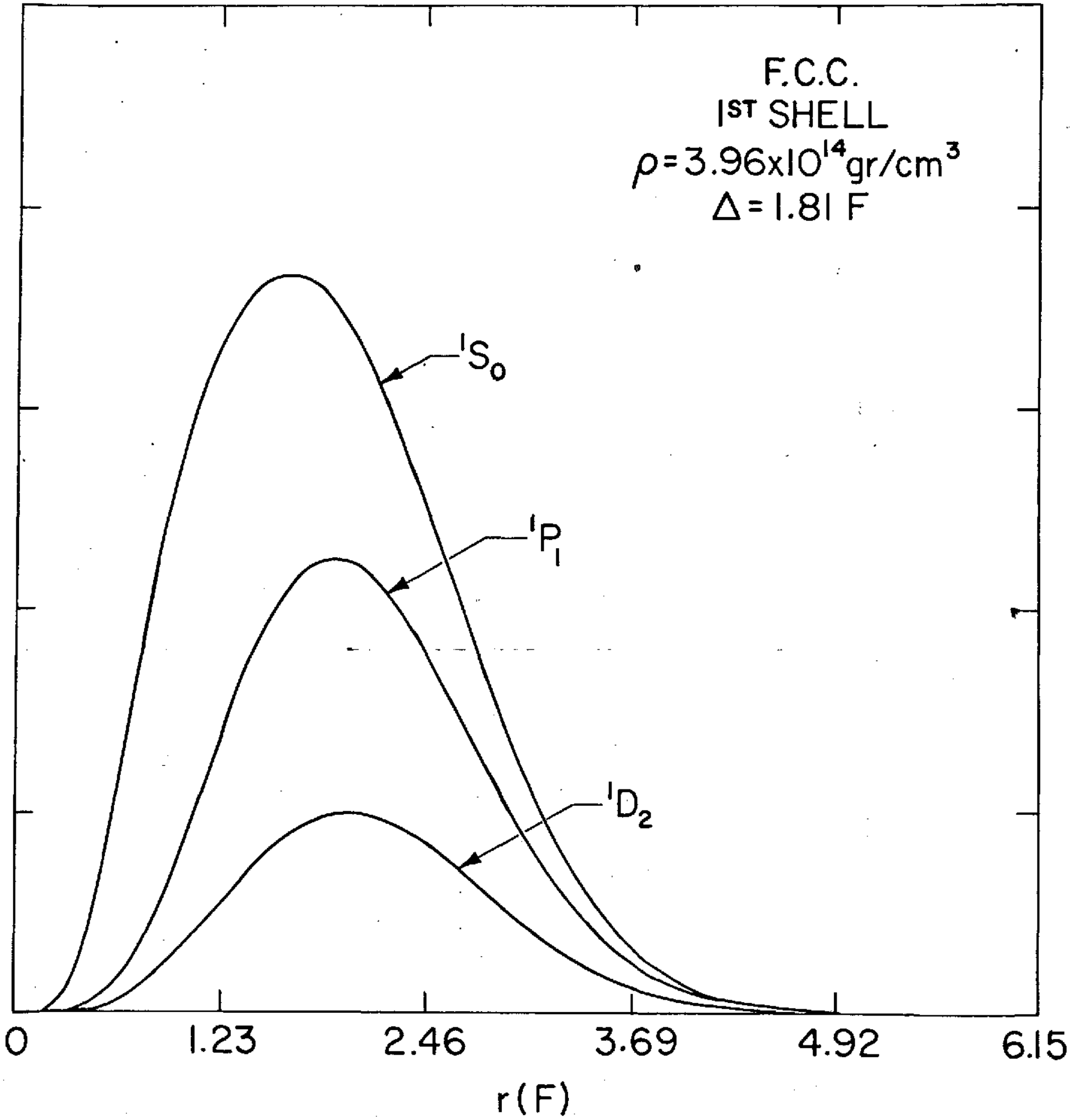
F.C.C.
1ST SHELL
ρ=3.96x10^14 gr/cm^3
Δ=1.81 F
1S0
1P1
1D2
0
1.23
2.46
3.69
4.92
6.15
r(F)

Fig. 3

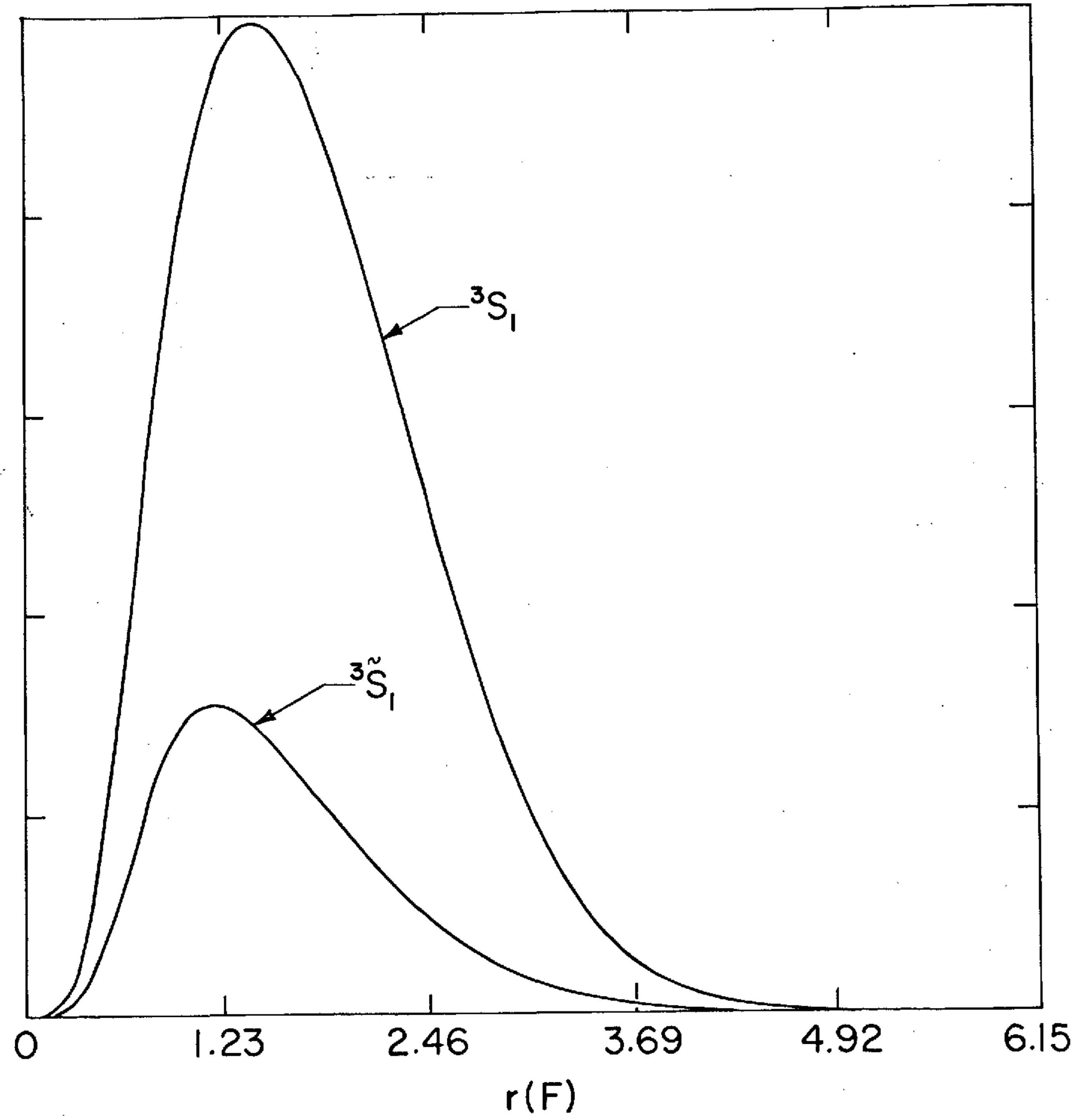

Fig. 4

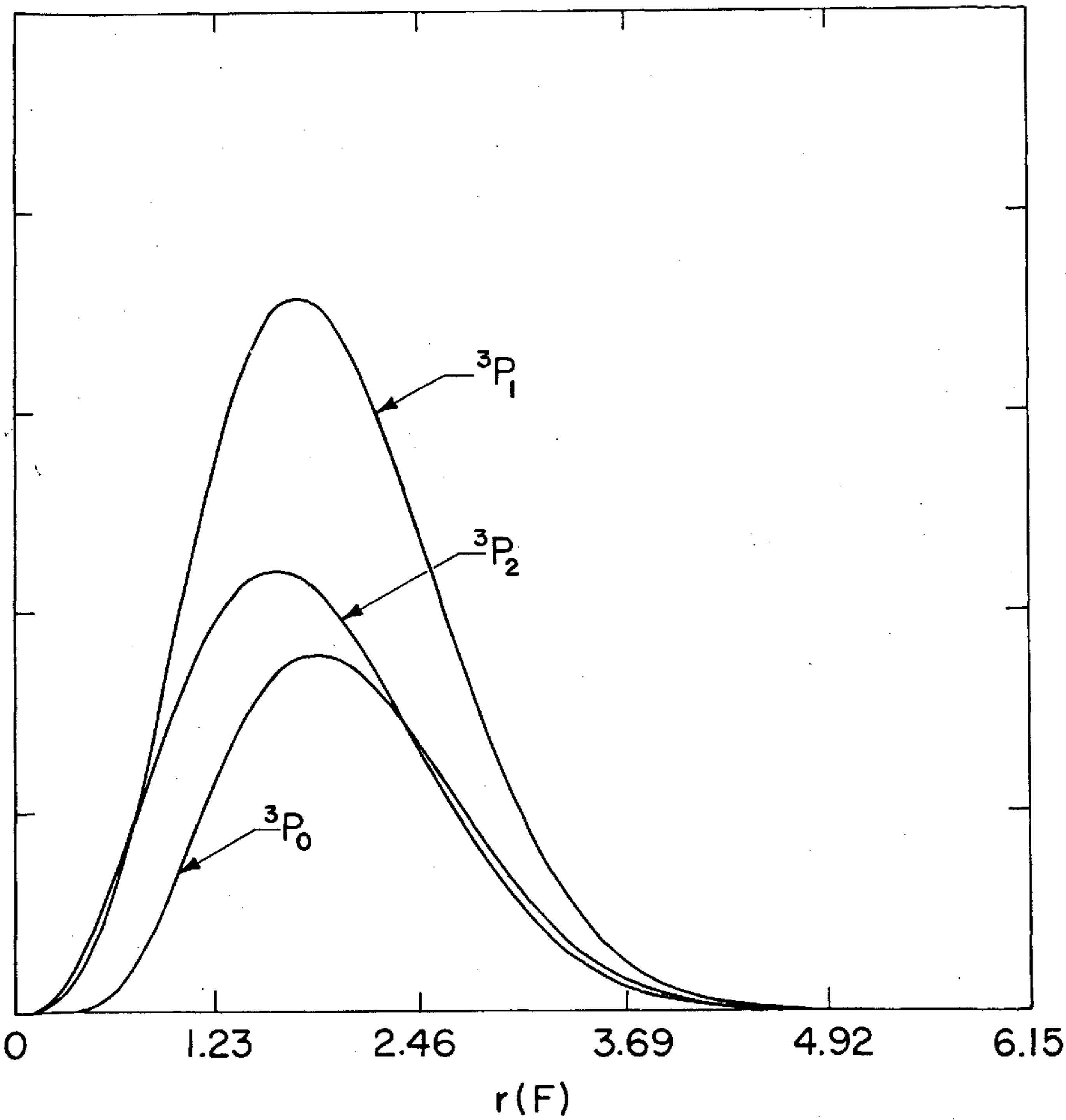

Fig. 5

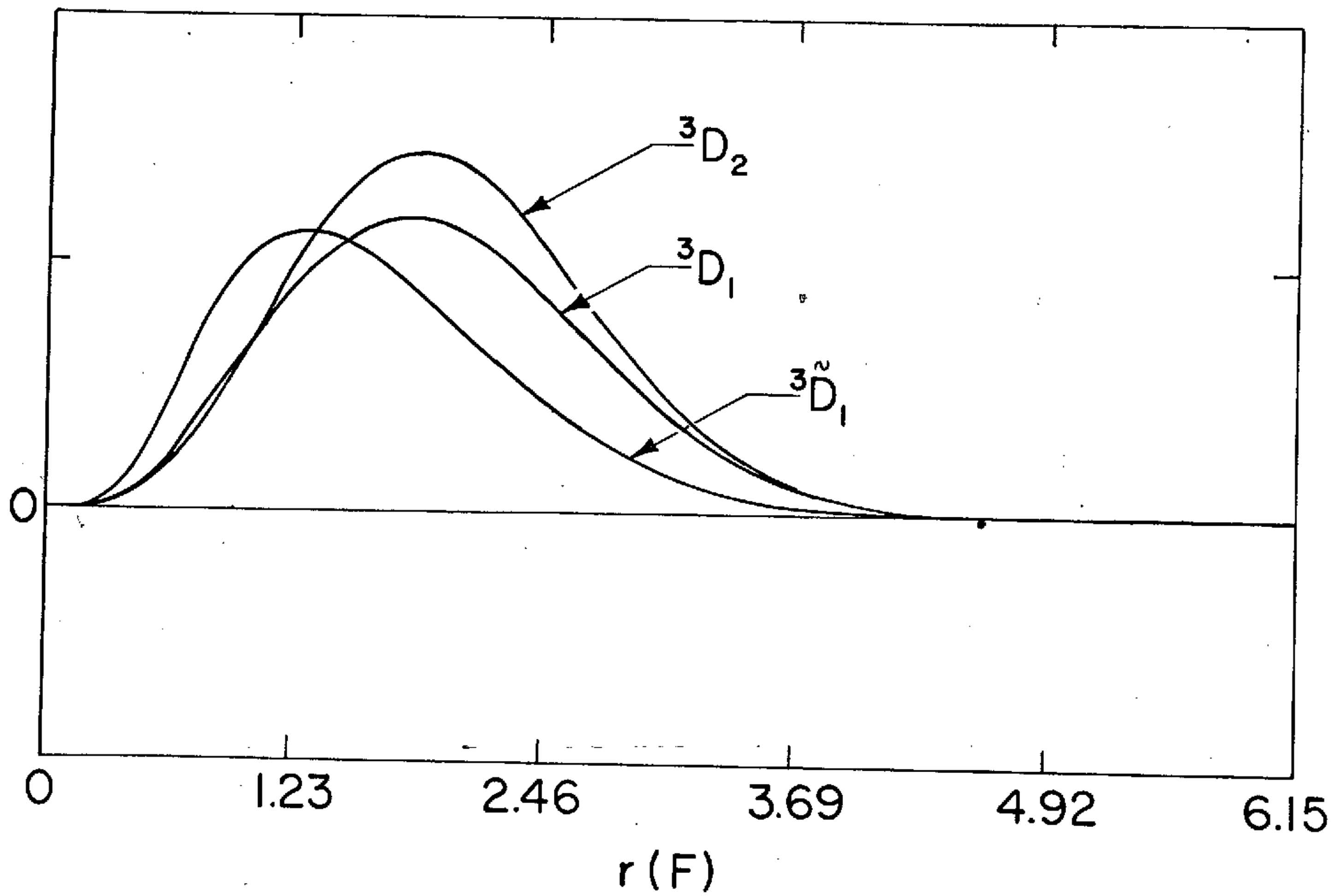

Fig. 6

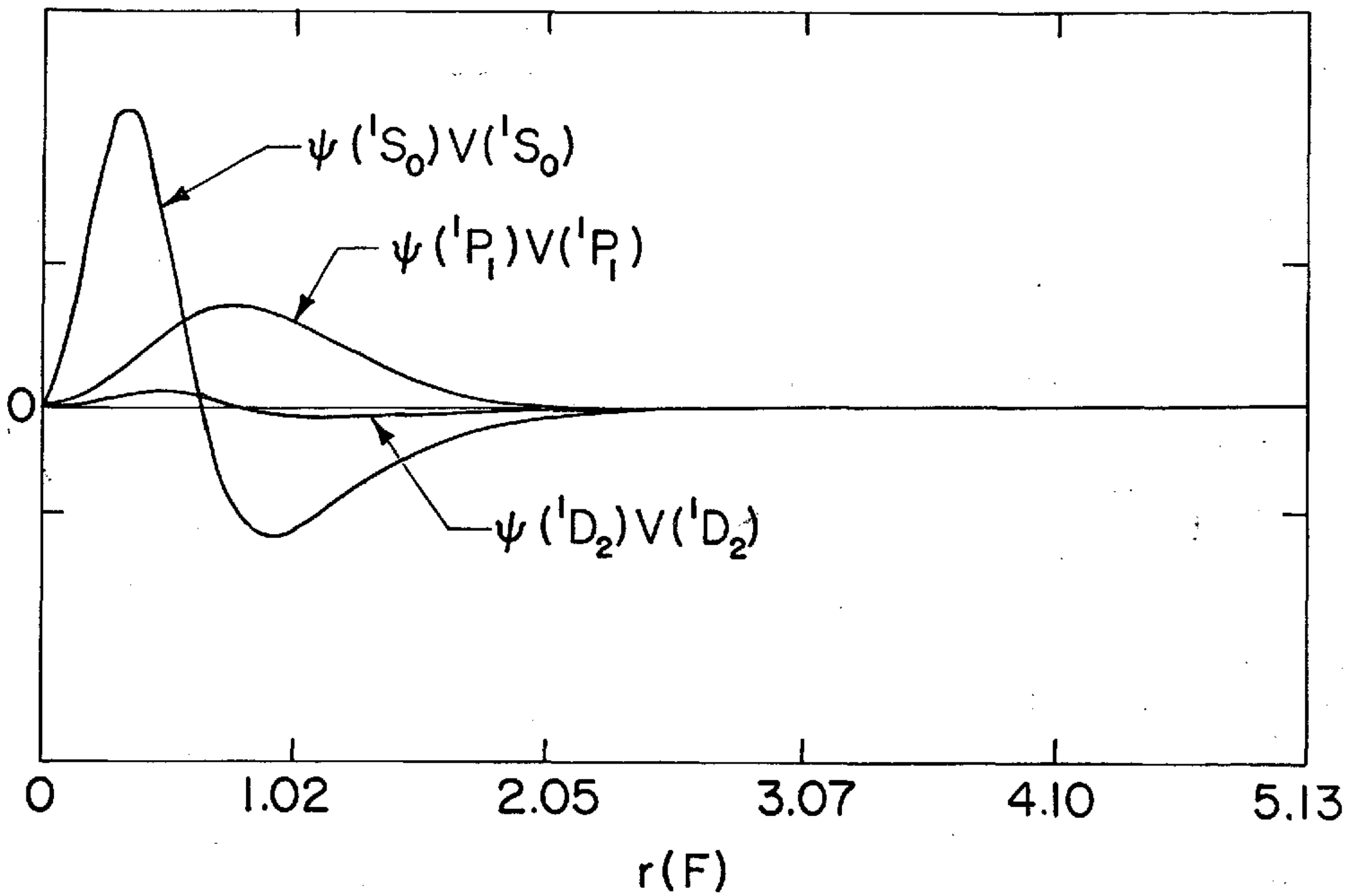

Fig. 7

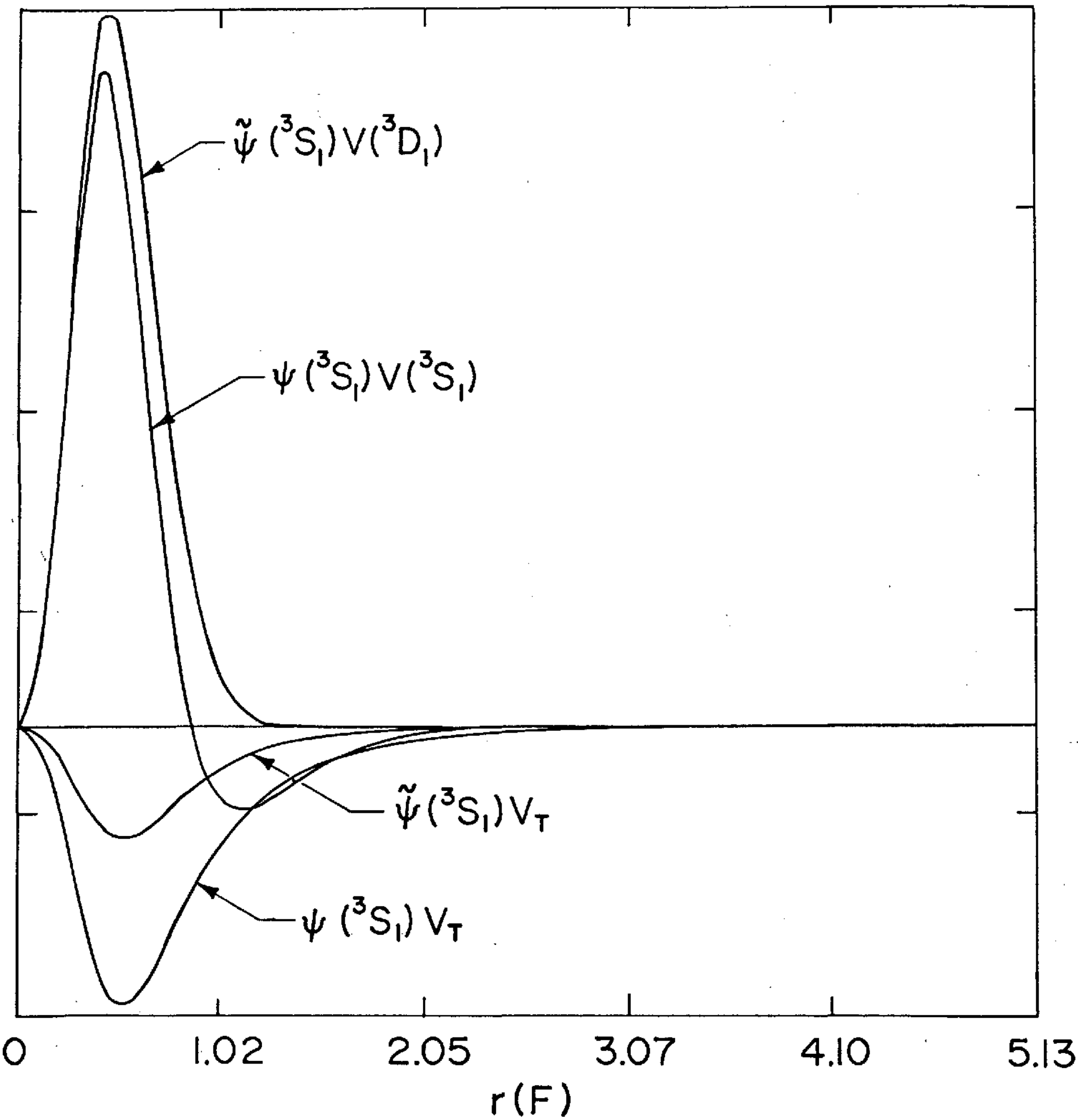

$\tilde{\psi}(^3S_1)V(^3D_1)$
$\psi(^3S_1)V(^3S_1)$
$\tilde{\psi}(^3S_1)V_T$
$\psi(^3S_1)V_T$
0
1.02
2.05
3.07
4.10
5.13
r(F)

Fig. 8

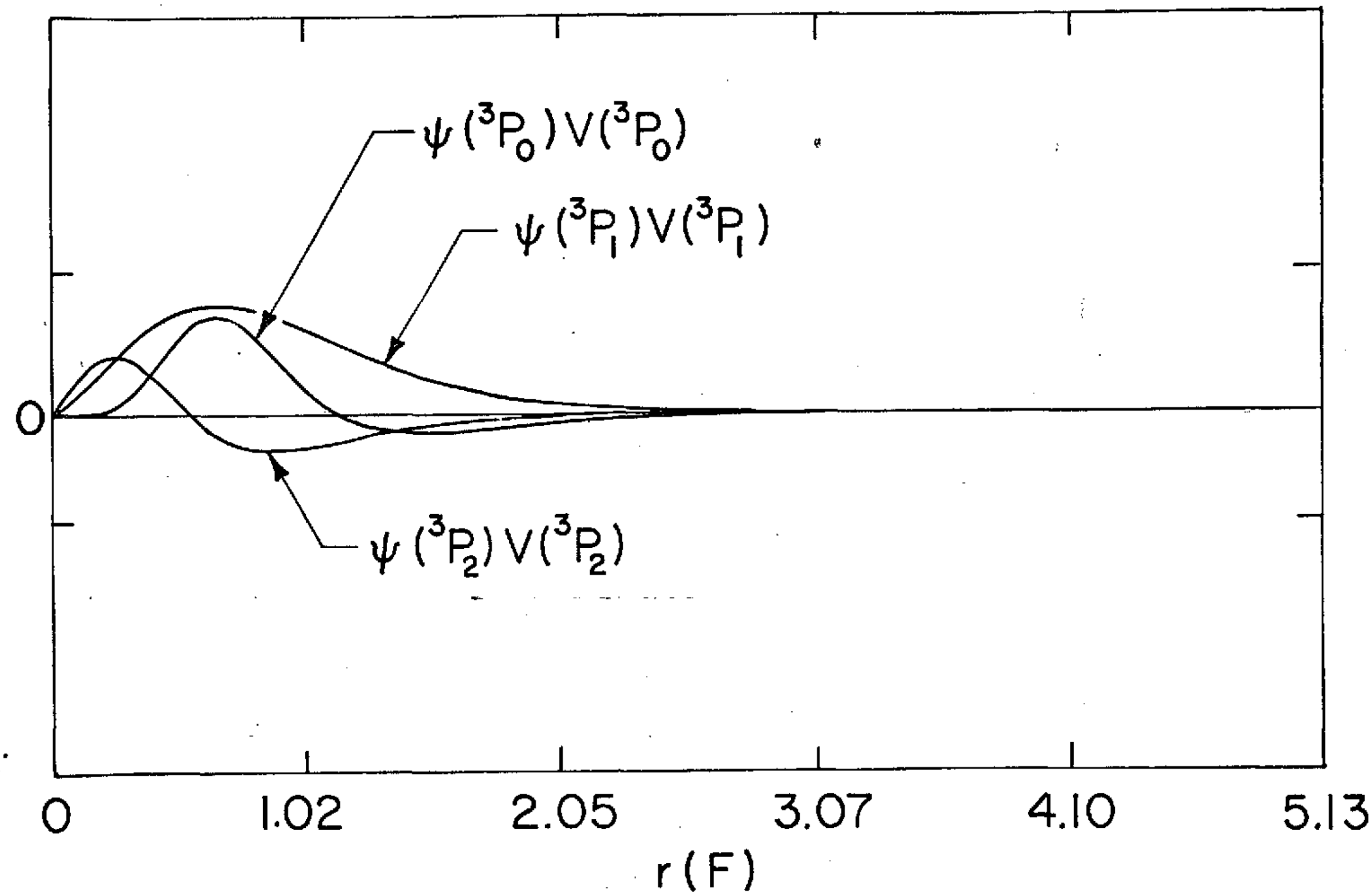

Fig. 9

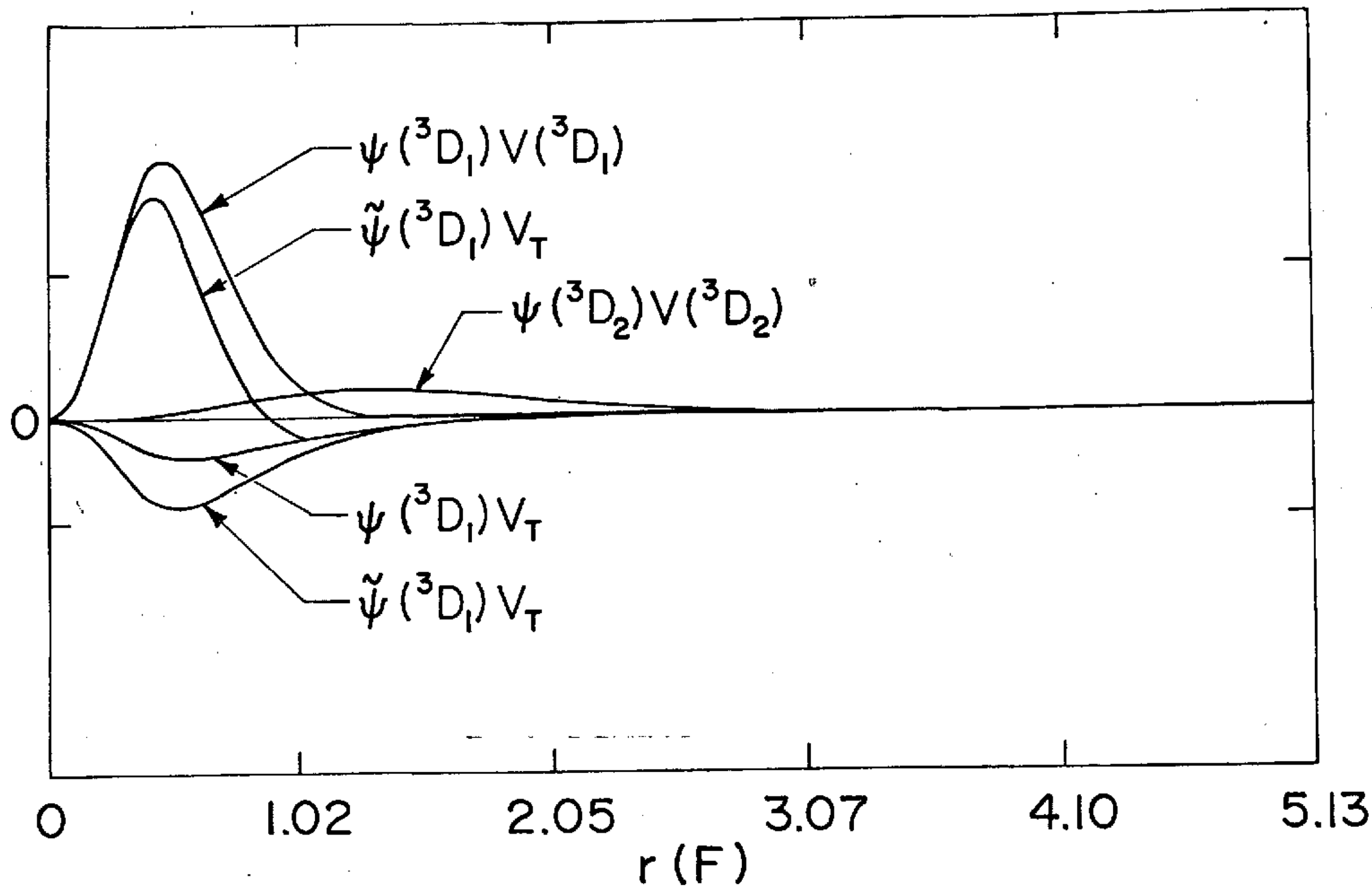
ψ (³D₁) V(³D₁)
ψ̃ (³D₁) V_T
ψ (³D₂) V(³D₂)
ψ (³D₁) V_T
ψ̃ (³D₁) V_T
0
0
1.02
2.05
3.07
4.10
5.13
r (F)

Fig. 10

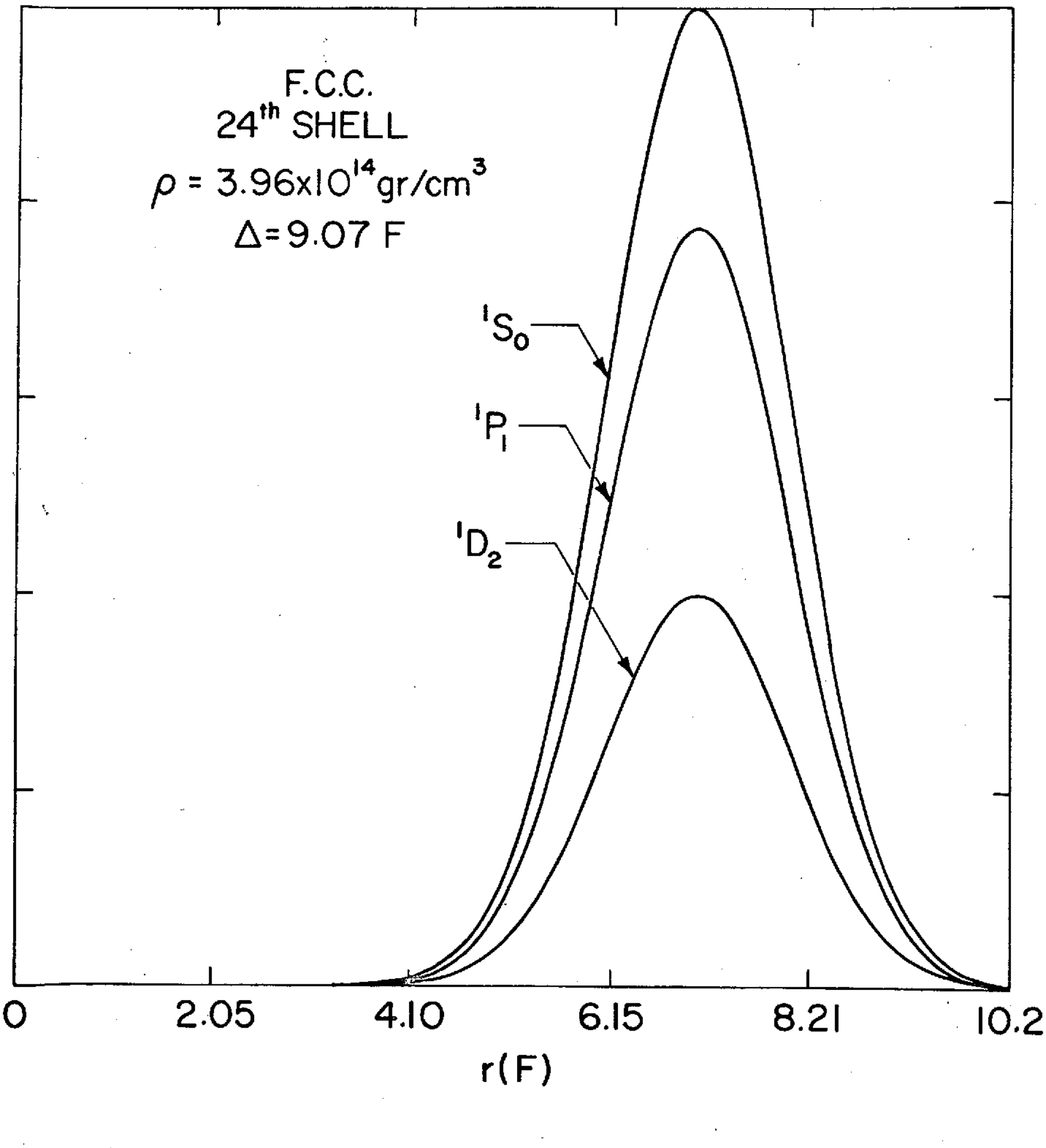
F.C.C.
24th SHELL
ρ = 3.96x10^14 gr/cm^3
Δ=9.07 F
1S0
1P1
1D2
0
2.05
4.10
6.15
8.21
10.2
r(F)

Fig. 11

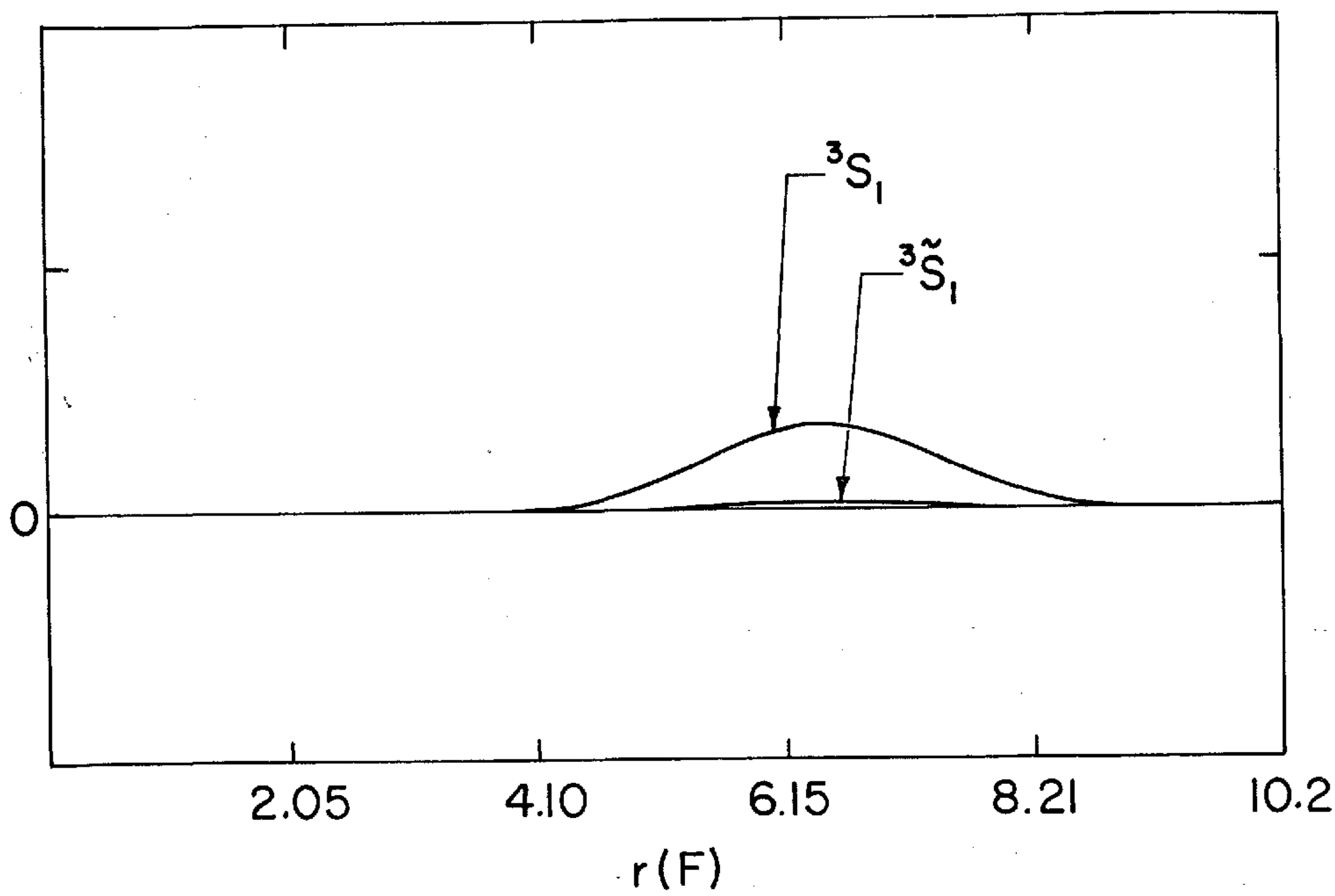

Fig. 12

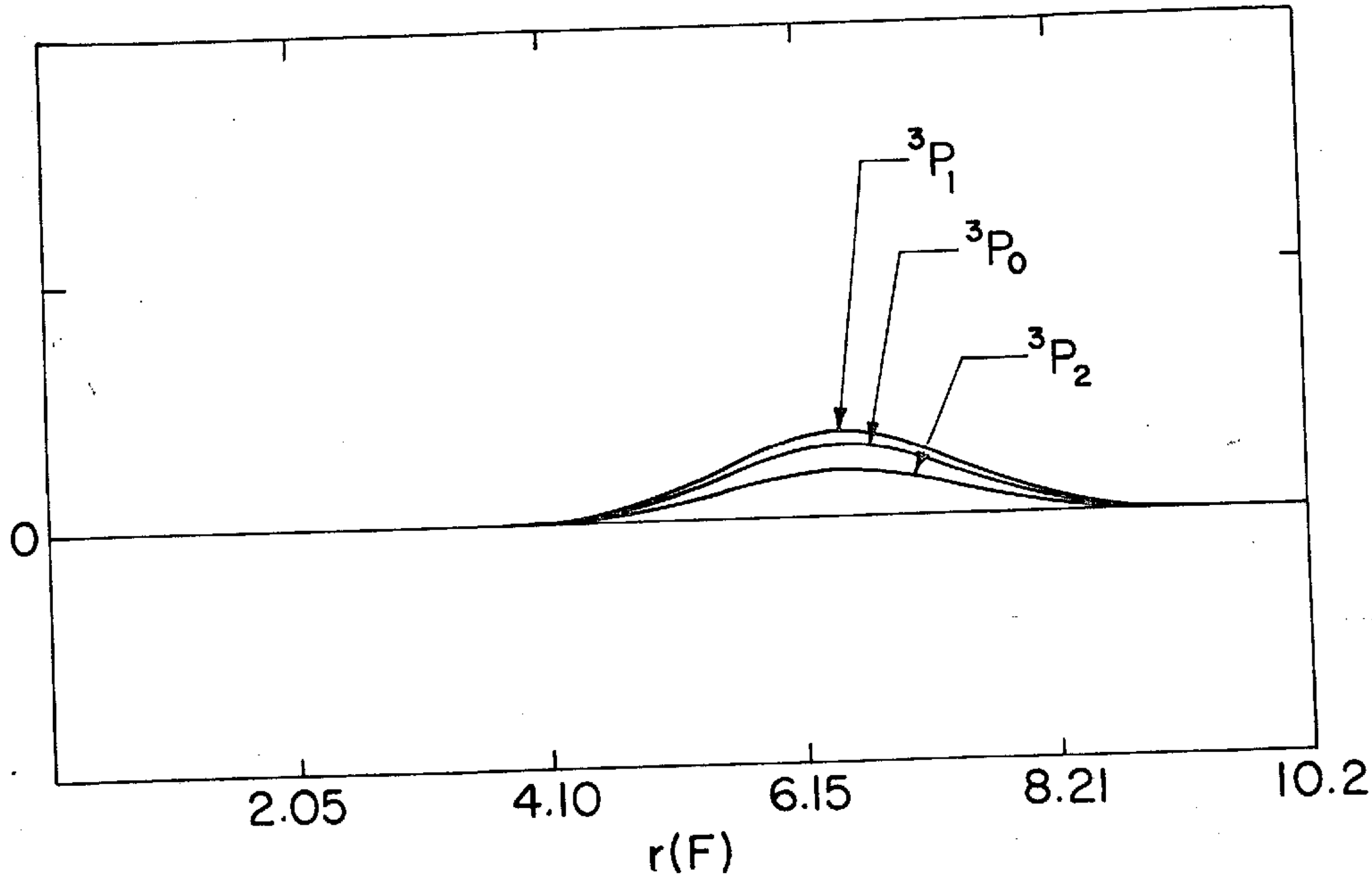

Fig. 13

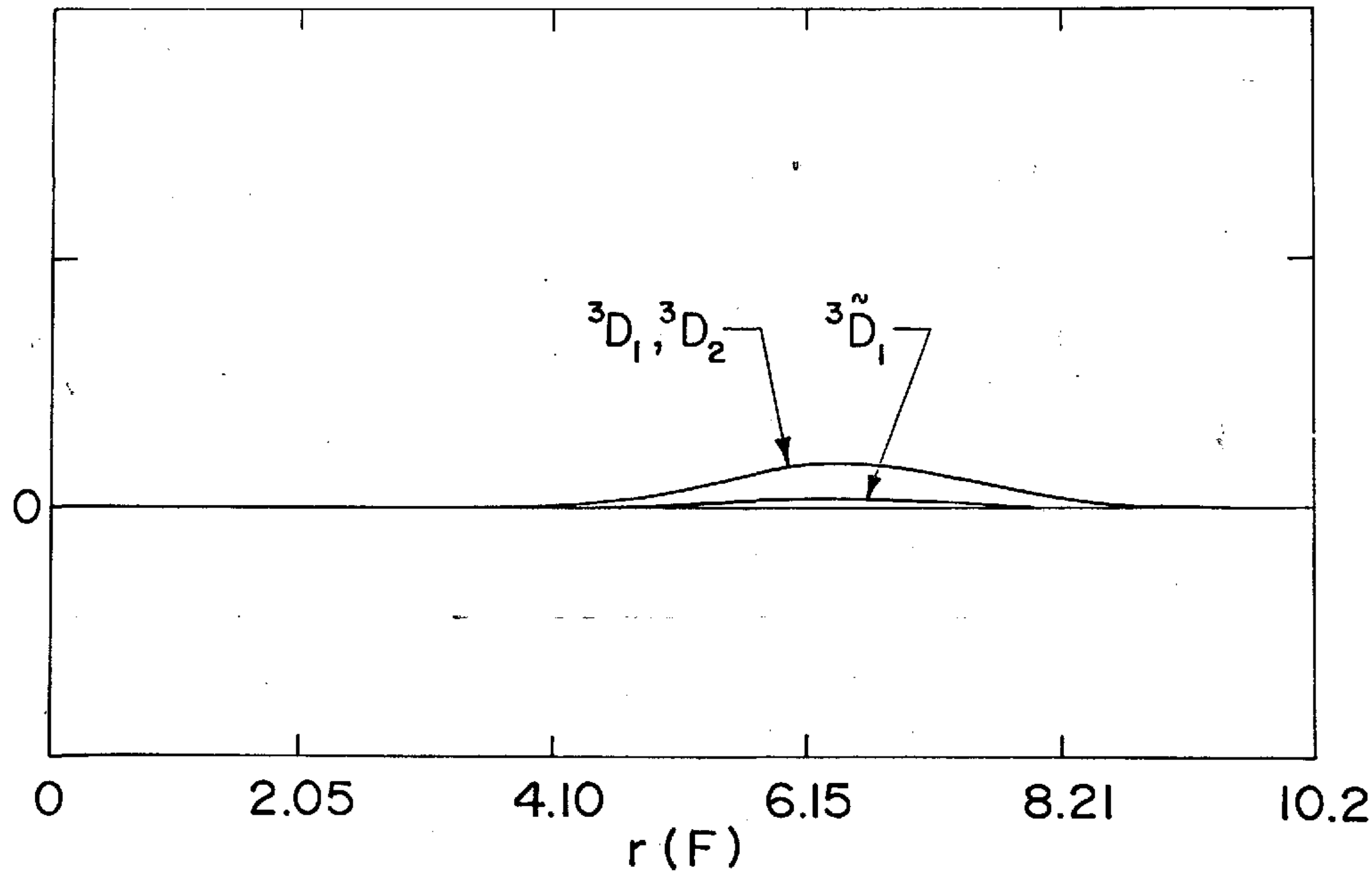

Fig. 14

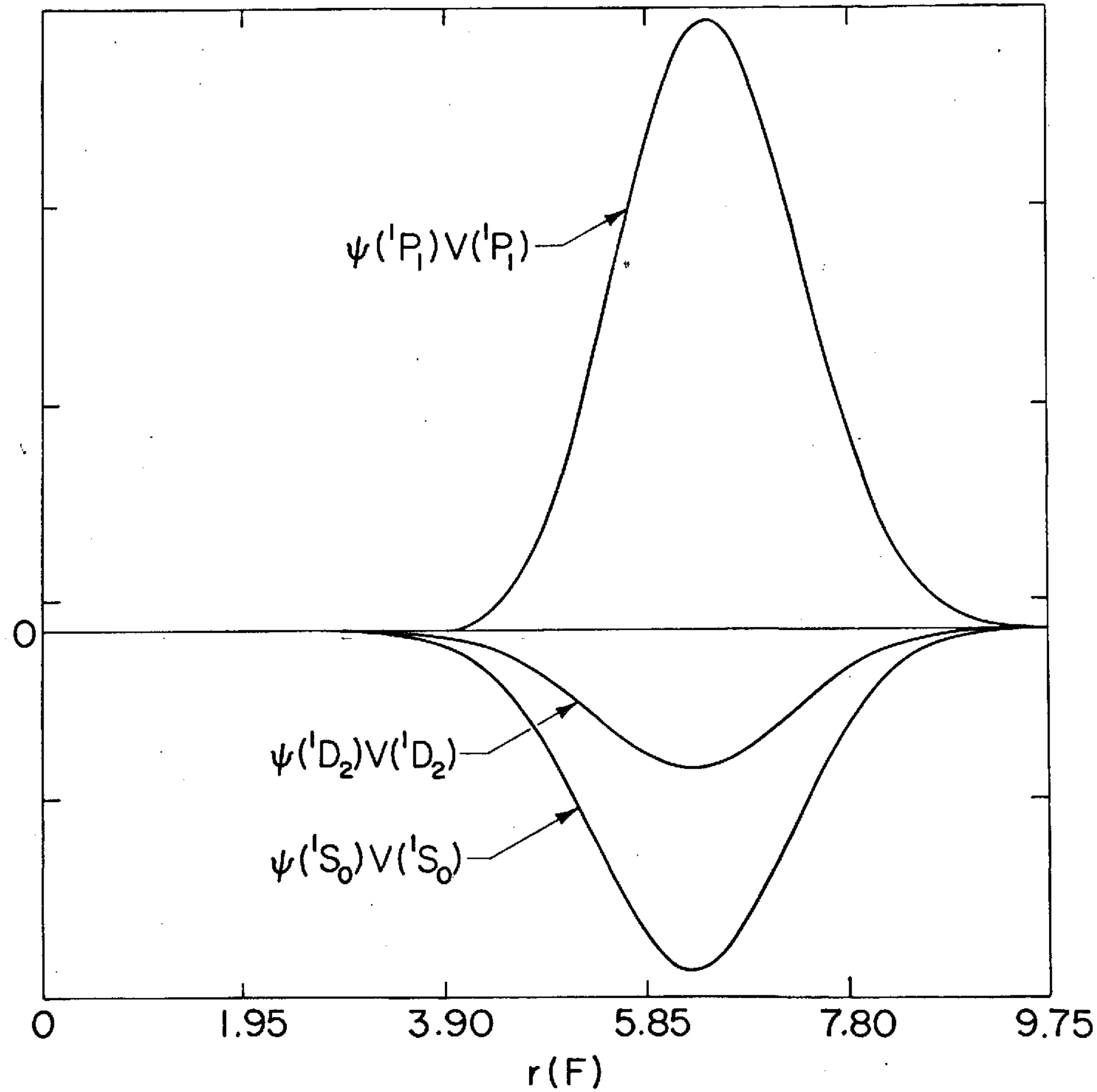

Fig. 15

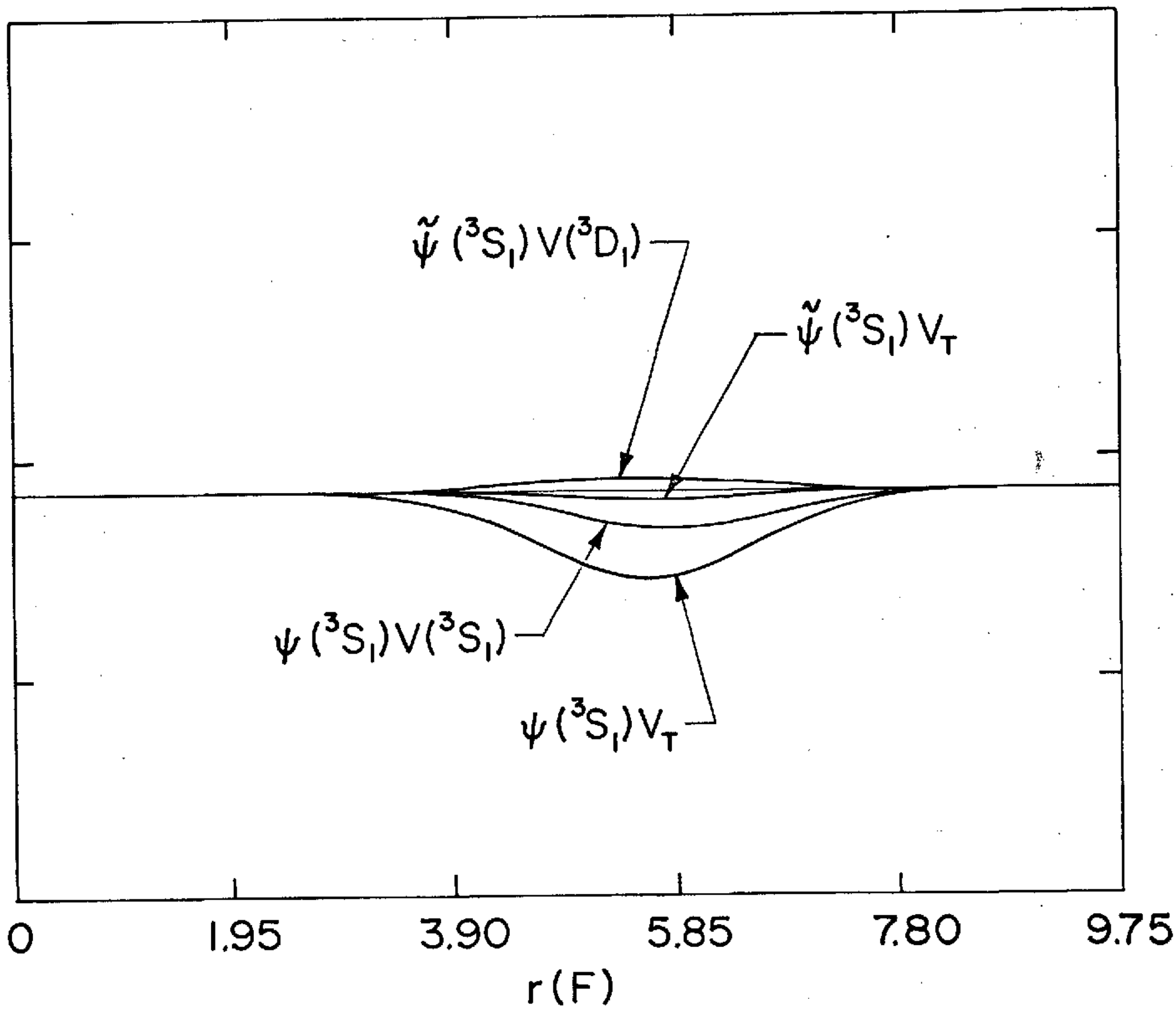
$\tilde{\psi}(^3S_1)V(^3D_1)$
$\tilde{\psi}(^3S_1)V_T$
$\psi(^3S_1)V(^3S_1)$
$\psi(^3S_1)V_T$
0
1.95
3.90
5.85
7.80
9.75
r(F)

Fig. 16

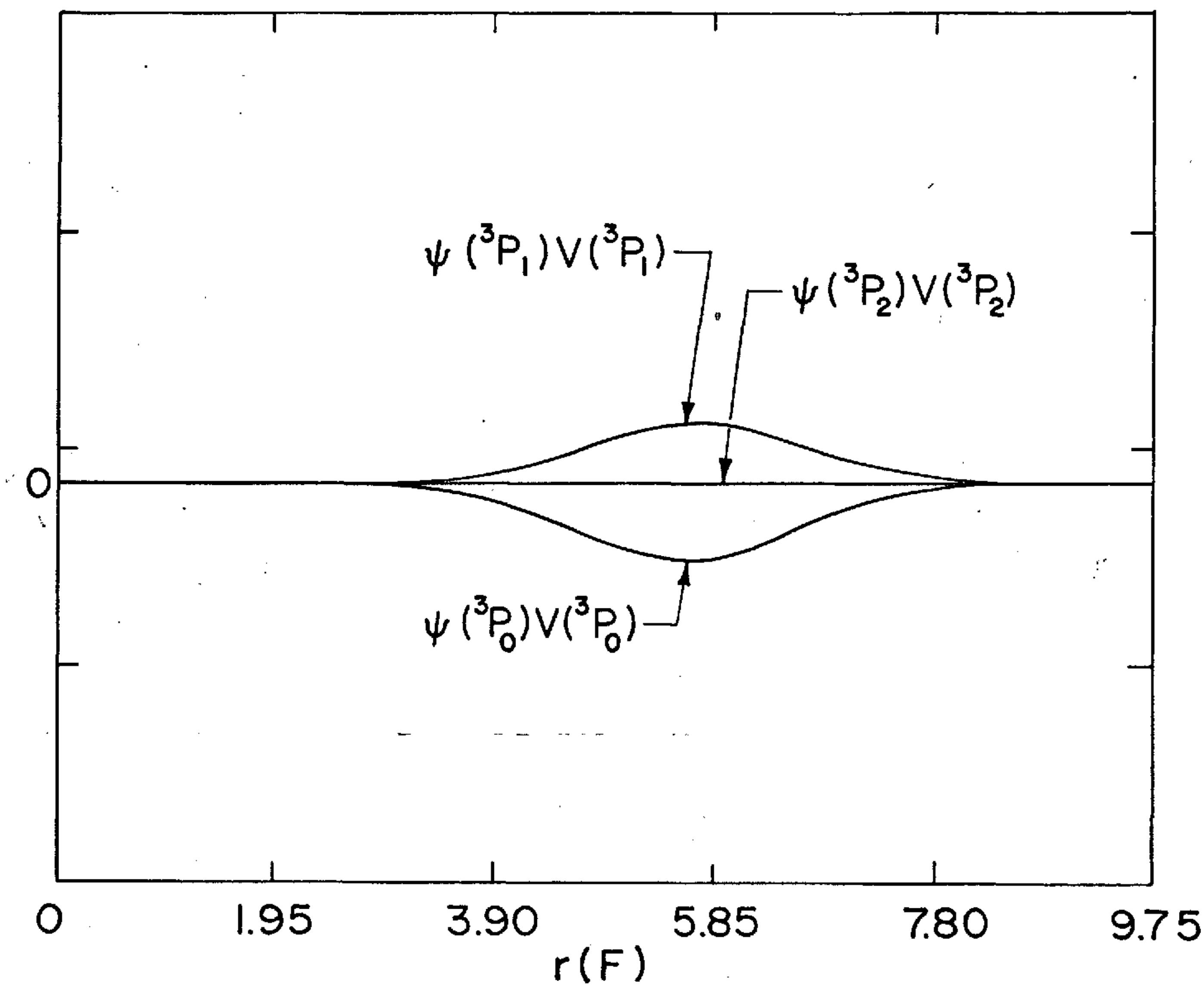

Fig. 17

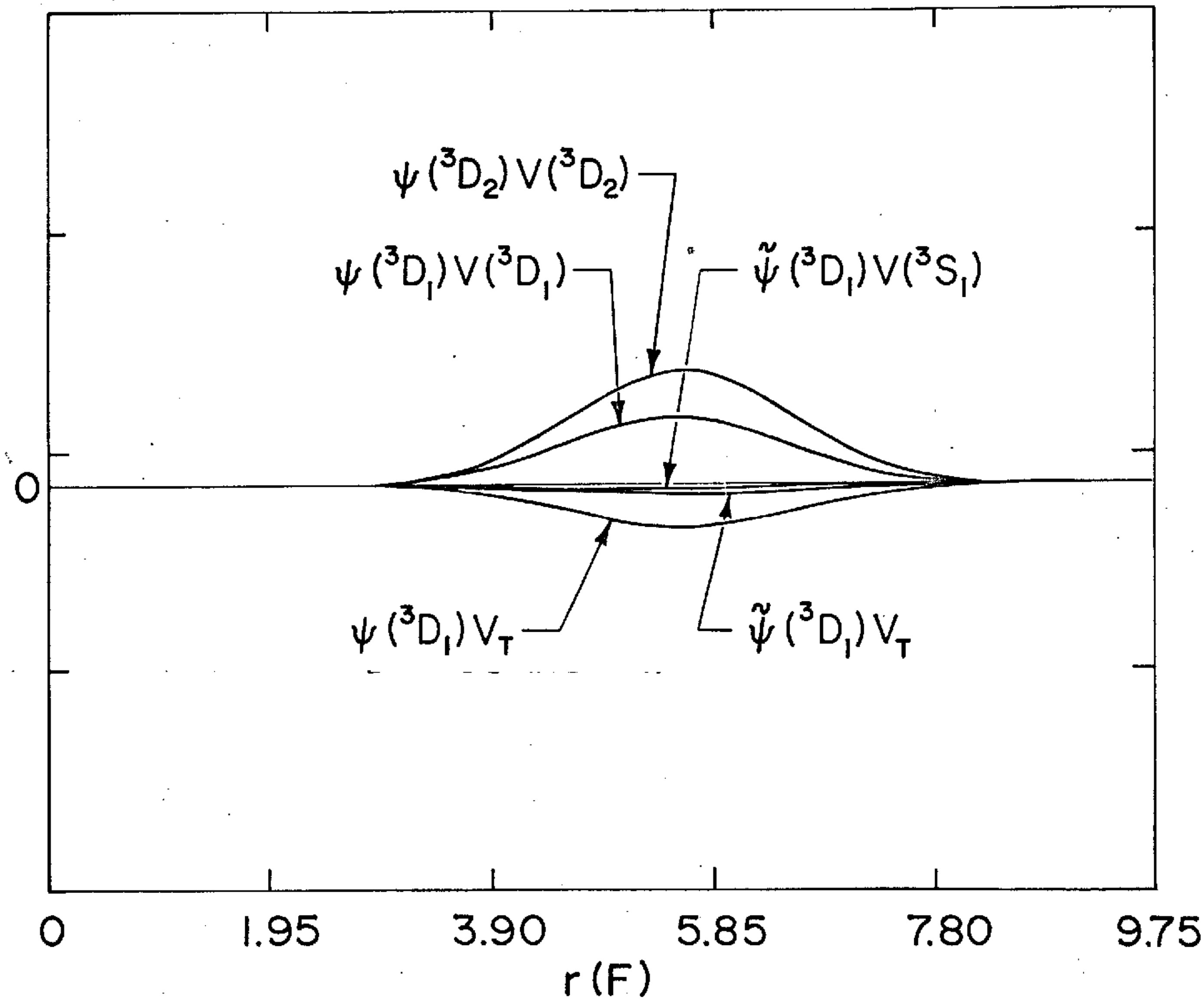
$\psi(^3D_2)V(^3D_2)$
$\psi(^3D_1)V(^3D_1)$
$\tilde{\psi}(^3D_1)V(^3S_1)$
$\psi(^3D_1)V_T$
$\tilde{\psi}(^3D_1)V_T$
0
0
1.95
3.90
5.85
7.80
9.75
r (F)

Fig. 18

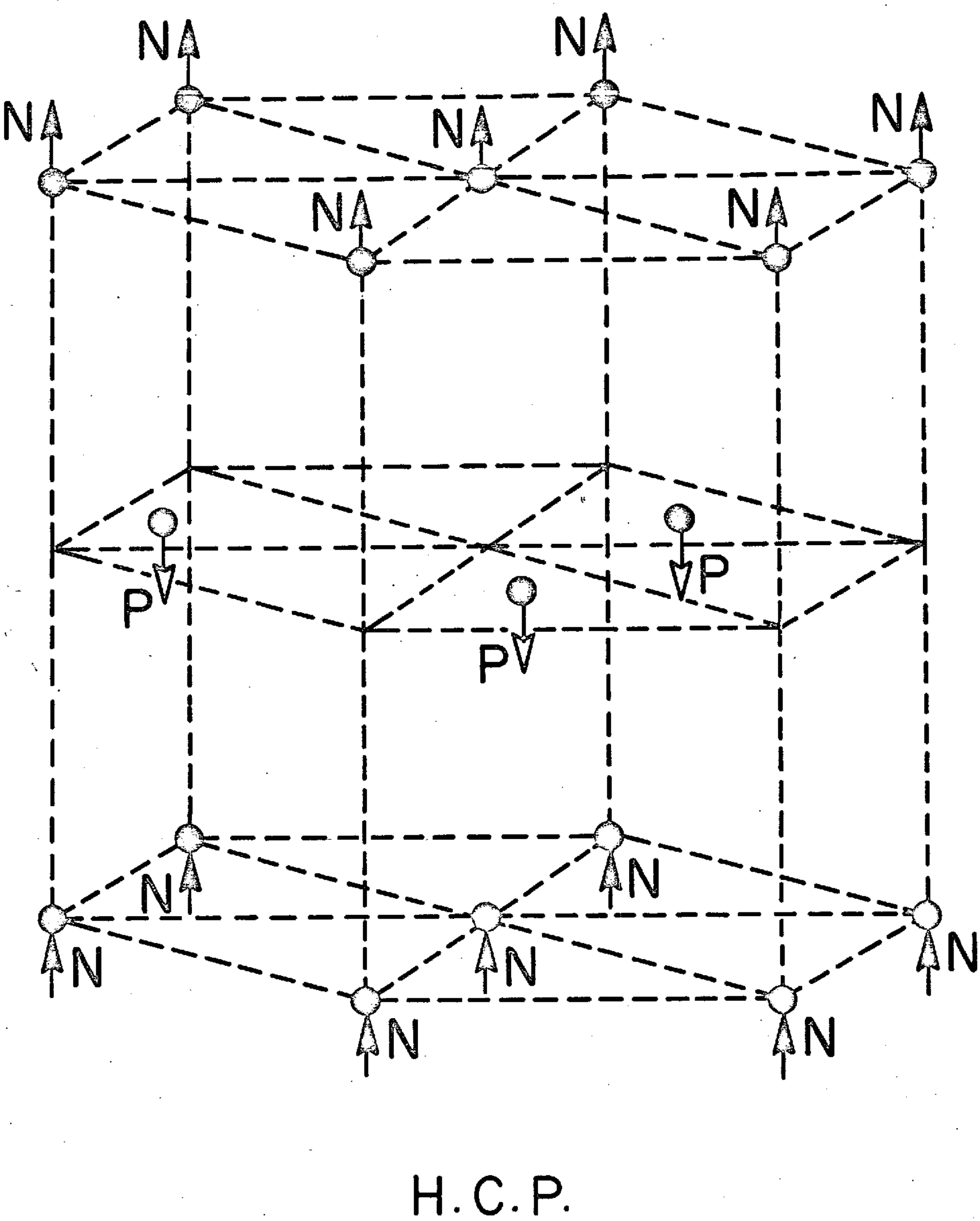

Fig. 19